Bioorg. Med. Chem. 40 (2021) 116185

Contents lists available at ScienceDirect

Bioorganic & Medicinal Chemistry

journal homepage: www.elsevier.com/locate/bmc

Novel hybrid conjugates with dual estrogen receptor α degradation and histone deacetylase inhibitory activities for breast cancer therapy

Chenxi Zhao [a], Chu Tang [b], Changhao Li [a], Wentao Ning [b], Zhiye Hu [b], Lilan Xin [b], Hai-Bing Zhou [b,*], Jian Huang [a,*]

[a] Hubei Key Laboratory of Cell Homeostasis, College of Life Sciences, Wuhan University, Wuhan 430072, China
[b] Hubei Provincial Key Laboratory of Developmentally Originated Disease, Frontier Science Center for Immunology and Metabolism, Key Laboratory of Combinatorial Biosynthesis and Drug Discovery (Wuhan University), Ministry of Education, Wuhan University School of Pharmaceutical Sciences, Wuhan 430071, China

ARTICLE INFO

Keywords:
Estrogen receptor α
Histone deacetylase
Breast cancer
Dual-functional conjugates
Protein degradation
Antiproliferative activity

ABSTRACT

Hormone therapy targeting estrogen receptors is widely used clinically for the treatment of breast cancer, such as tamoxifen, but most of them are partial agonists, which can cause serious side effects after long-term use. The use of selective estrogen receptor down-regulators (SERDs) may be an effective alternative to breast cancer therapy by directly degrading ERα protein to shut down ERα signaling. However, the solely clinically used SERD fulvestrant, is low orally bioavailable and requires intravenous injection, which severely limits its clinical application. On the other hand, double- or multi-target conjugates, which are able to synergize antitumor activity by different pathways, thus may enhance therapeutic effect in comparison with single targeted therapy. In this study, we designed and synthesized a series of novel dual-functional conjugates targeting both ERα degradation and histone deacetylase inhibiton by combining a privileged SERD skeleton 7-oxabicyclo[2.2.1]heptane sulfonamide (OBHSA) with a histone deacetylase inhibitor side chain. We found that substituents on both the sulfonamide nitrogen and phenyl group of OBHSA unit had significant effect on biological activities. Among them, conjugate **16i** with *N*-methyl and naphthyl groups exhibited potent antiproliferative activity against MCF-7 cells, and excellent ERα degradation activity and HDACs inhibitory ability. A further molecular docking study indicated the interaction patterns of these conjugates with ERα, which may provide guidance to design novel SERDs or PROTAC-like SERDs for breast cancer therapy.

1. Introduction

Breast cancer is the most common cancer as well as one of the leading causes of death of women.[1,2] In 2020, approximately 276,000 new breast cancer cases and at least 40,000 deaths are expected among women in the United States. That accounts for 30% of predicted all cancer incidence of women in the year 2020.[3] Among them, nearly 79% breast cancer patients were diagnosed with estrogen receptor (ER) positive,[4,5] which is a critical transcription factor in the development of breast cancer.[6–8] Accordingly, endocrine therapy targeting ER has become an important therapeutic strategy for breast cancer.[5,9–11] For example, five-year's adjuvant treatment with tamoxifen, a selective estrogen receptor modulator (SERM), on early stage breast cancer patients could reduce the risk of breast cancer recurrence and death by about 40% and 30%, respectively.[5,12,13] Unfortunately, SERMs are the partial agonists.[14,15] Although SERMs act as antagonists in the breast cancer, while which act as a mixture of agonists and antagonists in the uterus,[16] and long-term use of these drugs can have serious side effects, such as increasing the risk of endometrial cancer, venous thrombosis and cognitive impairment.[17–19] In contrast, selective estrogen receptor down-regulators (SERDs) have numerous advantages,[20] which can directly degrade ERα protein by activating the ubiquitination pathway.[21] Fulvestrant is the first approved-SERD by the FDA,[22,23] which has been applied to treat tamoxifen-resistance breast cancer. However, fulvestrant is low orally bioavailable and requires intravenous injection, which severely limits its clinical application.[24] Therefore, it is urgent to develop novel SERDs to treat breast cancer.

In recent years, our group has been working on the development of ER ligands for treatment of breast cancer, and has obtained a number of ligands with excellent biological activity. Among them, OBHS (compound **1**, Fig. 1) was one of the most potential.[25] which exhibited high binding affinity and significant antiproliferative effects on MCF-7 cells,

* Corresponding authors. Tel.: +862768759586 (H.-B. Zhou). Tel.: +862768753582 (J. Huang).
E-mail addresses: zhouhb@whu.edu.cn (H.-B. Zhou), jianhuang@whu.edu.cn (J. Huang).

https://doi.org/10.1016/j.bmc.2021.116185
Received 26 January 2021; Received in revised form 17 April 2021; Accepted 26 April 2021
Available online 1 May 2021

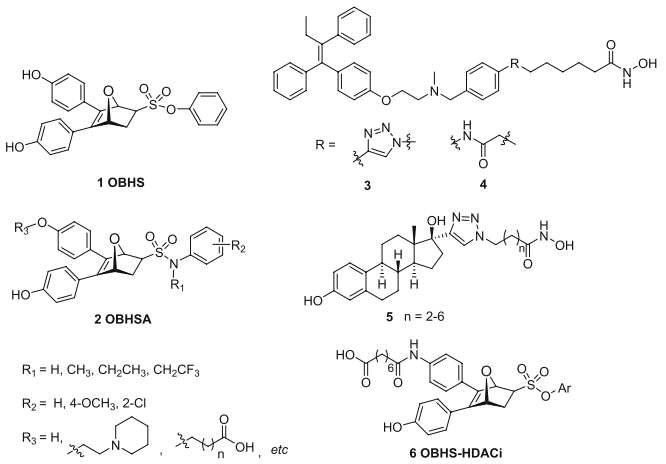

Fig. 1. The structures of OBHS, OBHSA, Tam-HDACi, EED-HDACi and OBHS-HDACi derivatives.

while the ER subtype selectivity was modest, and was a partial ERα agonist. Surprisingly, when the sulfonate of OBHS was changed to sulfonamide (OBHSA, **2**, Fig. 1), which became an ERα full antagonist and could slightly induce ERα degradation.[26,27] Subsequently, we further found that introduction of side chain on the phenyl ring of sulfonamide of OBHSA could significantly increase the degradation effect of ERα (compound **2**, Fig. 1).[28,29] Especially, the SERDs that contain the OBHSA core structure and different polar side chain could simply mimic the degrons of proteolysis targeting chimera (PROTAC) and effectively inhibit MCF-7 cell proliferation and demonstrated good ERα degradation efficacy.[28]

Considering that cancer is a multifactorial, multi-gene disease,[30–32] single targeted therapy is often difficult to achieve the desired therapeutic effect,[33,34] thus the attachment of the second anti-tumor component to phenyl ring of sulfonamide of OBHSA can not only improve the ERα degradation effect, but also may endow the synthesized compound with double-targeting property,[35] which are able to synergize antitumor activity by different pathways and finally enhance the therapeutic effects. In recent years, a number of dual-acting compounds targeting both ER and another target such as VEGFR-2,[36] IGF1R,[37] tubulin,[38] or NF-κB *etc*, have been synthesized.[35,39] It is well known that aberrant histone deacetylase (HDAC) activity is related to many cancers, including breast cancer. Vorinostat (SAHA) is one of HDAC inhibitors, which was approved by FDA in 2006 to treat *T*-cell lymphoma. In 2013, Oyelere *et al* have covalently linked SAHA and its derivatives to tamoxifen (compound **3** and **4**, Fig. 1) and 17α-ethinylestradiol (compound **5**, Fig. 1) to obtain the Tam-HDACi and EED-HDACi conjugates, respectively. Both Tam-HDACi and EED-HDACi conjugates retain independent estrogen receptor binding ability and anti-HDAC activities. Unfortunately, Tam-HDACi conjugates showed small *in vitro* therapeutic index (IVTI).[40] In previous studies, we found that the OBHS-HDACi conjugates **6**, which coupling ER ligand OBHS with histone deacetylase (HDAC) inhibitor (Fig. 1) could significantly improve anti-breast cancer activity compared to OBHS alone, and show no toxicity toward normal cells.[41] However, these conjugates had no ER degradation activity.

Hence, in this study, we report the design and biological evaluation of novel dual-acting agents targeting both ER and histone deacetylase (named OBHSA-HDACi conjugates, Fig. 2) by introducing HDAC inhibitor unit into OBHSA scaffold. The OBHSA-HDACi conjugates of this design exhibited significantly ERα degradation and histone deacetylase inhibitory activities, and synergetic antiproliferation activity against MCF-7 cell lines.

2. Results and discussion

2.1. Chemical Synthesis

OBHSA-HDACi conjugates were synthesized by Diels-Alder cycloaddition of furan derivatives **7** with various dienophiles (Scheme 2). The intermediates 8-(4-(4-(4-hydroxyphenyl)furan-3-yl)-phenylamino)-8-oxooctanoic acid **7** were prepared according to our previously described methodology.[25,41]

Tertiary sulfonamide dienophiles (*N*-substituents CH_3, CH_2CH_3, CH_2CF_3) **12a-i**, **14a-i** and **15a-f** were synthesized from various commercially available substituted anilines (Scheme 1A and 1B). Anilines containing different electron-donating or electron-withdrawing groups were reacted with acetic anhydride to afford compound **9a**. Then **9a** was methylated with iodomethane giving compound **10**. After that, the acetyl group was removed in the presence of hydrochloric acid to get compound **11**. Finally, with NaOH as the base, *N*-methylsulfonamide dienophile **12a-i** was obtained by reacting with 2-chloroethanesulfonyl chloride. On the other hand, *N*-ethyl or trifluoroethylsulfonamide dienophiles **14a-i** and **15a-f** were obtained through three steps. Anilines were reacted with trifluoroacetic anhydride to afford compound **9b**. Subsequently, the carbonyl group of **9a** or **9b** were reduced to methylene with borane-methyl sulfide complex as reductant. Finally, compound **13a** or **13b** reacted with 2-chloroethanesulfonyl chloride to afford target dienophiles **14a-i** and **15a-f**.

With some success of the OBHS-HDACi conjugates in our previous work,[41] we observed that the conjugates obtained by introducing suberic acid into OBHS scaffold had a higher RBA value, stronger antagonistic activity and more effective inhibition activity against breast cancer MCF-7 cell line than the ones with SAHA. Therefore, when designing the OBHSA-HDACi conjugates, we focused on the synthesis of the conjugates with a suberic acid. Notably, there was a high stereoselectivity in the Diels-Alder reaction with a high yield (Scheme 2). The *exo* isomers were predominated and *endo* isomers were only trace. Thus, the *exo* isomers were used as racemates for biological study; the structures of conjugates were summarized in Table 1.

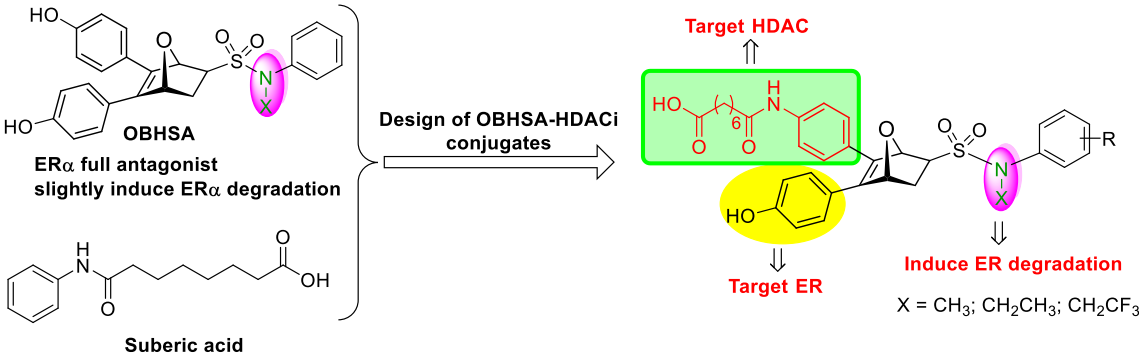

Fig. 2. Design of dual-acting OBHSA-HDACi conjugates.

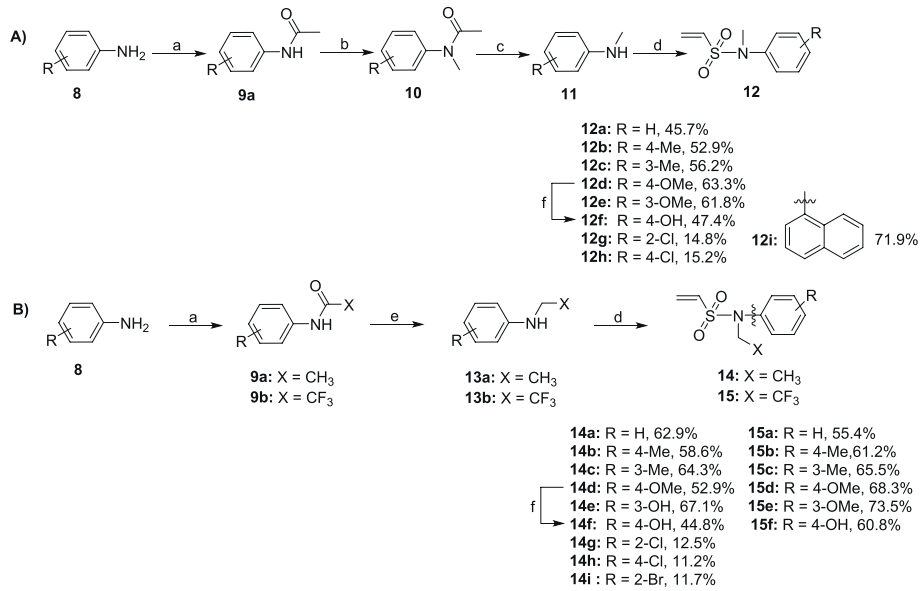

Scheme 1. Synthesis of dienophiles **12a-i**, **14a-i** and **15a-f**. Reagents and conditions: (a) acetic anhydride or trifluoroacetic anhydride, rt, 3 h; (b) NaH, CH_3I, THF, 0 °C, 4 h; (c) 10% HCl, $HO(CH_2)_2OH$, rt, 3 h; (d) 2-chloroethanesulfonyl chloride, 20% NaOH, DCM, 0 °C, 24 h; (e) $BH_3 \cdot SMe_2$, THF, 60 °C, 24 h; (f) BBr_3, DCM, −20 °C, 12 h.

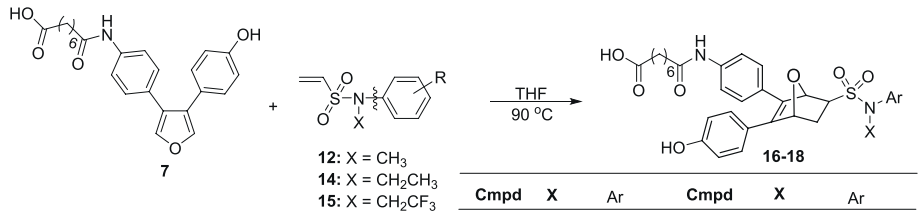

Cmpd	X	Ar	Cmpd	X	Ar
16a	CH_3	Ph	**17d**	CH_2CH_3	4-OMe-Ph
16b	CH_3	4-Me-Ph	**17e**	CH_2CH_3	3-OMe-Ph
16c	CH_3	3-Me-Ph	**17f**	CH_2CH_3	4-OH-Ph
16d	CH_3	4-OMe-Ph	**17g**	CH_2CH_3	2-Cl-Ph
16e	CH_3	3-OMe-Ph	**17h**	CH_2CH_3	4-Cl-Ph
16f	CH_3	4-OH-Ph	**17i**	CH_2CH_3	2-Br-Ph
16g	CH_3	2-Cl-Ph	**18a**	CH_2CF_3	Ph
16h	CH_3	4-Cl-Ph	**18b**	CH_2CF_3	4-Me-Ph
16i	CH_3	1-naphthyl	**18c**	CH_2CF_3	3-Me-Ph
17a	CH_2CH_3	Ph	**18d**	CH_2CF_3	4-OMe-Ph
17b	CH_2CH_3	4-Me-Ph	**18e**	CH_2CF_3	3-OMe-Ph
17c	CH_2CH_3	3-Me-Ph	**18f**	CH_2CF_3	CH_2-Ph

Scheme 2. Synthesis of OBHSA-HDACi conjugates **16**–**18**.

2.2. Binding affinity of OBHSA-HDACi conjugates

A competitive fluorescence polarization assay was used to evaluate the binding affinities of these conjugates **16a-i**, **17a-i** and **18a-f**, and the results were reported in Table 2.

Generally speaking, most OBHSA-HDACi conjugates exhibited good to moderate relative binding affinity (RBA) values as well as good selectivity for ERα. In these three series of compounds, *N*-methyl substituted compounds **16a-i** displayed higher affinity than *N*-ethyl or trifluoroethyl substituted compounds **17a-i** and **18a-f**. In fact, the RBA values of *N*-ethyl substituted compounds did not exceed 2.5% (Table 2, entries 10–18), and *N*-trifluoroethyl substituted compounds were even <1% (Table 2, entries 19–24). However, the substituents on phenyl ring of sulfonamide unit *N*-methyl substituted compounds have great influence on the RBA. Taking compound **16a** as an example, which has no substituents in phenyl unit, exhibited the highest ERα binding affinity as 13.07 among all the conjugates and good ERβ binding affinity as 6.00; yet, when the phenyl ring was substituted with electron-donating group, such as methyl, methoxyl, hydroxyl group, although they remained a moderate binding affinity, the RBA value was significantly reduced by 2–30 times (analogues **16b-f**, Table 2, entries 2–6). To our delight, introduction of 2-chloro group (compound **16g**) not only retained high ERα binding affinity (RBA: 11.6 vs 13.07) but also significantly improved ERα subtype selectivity (α/β: 1160 vs 2.17) compared to **16a**. While 2-chloro was changed to 4-chloro, a progressive decrease of ERα RBA value and subtype selectivity was observed (Table 2, entries 7–8, **16g** vs **16h**). Additionally, replacing the benzene ring of sulfonamide with a larger naphthyl group, RBA value was also decreased significantly (Table 2, entries 1 vs 9). In addition, in order to compare with previously reported OBHS-HDACi conjugates[41], we chose two compounds **OBHS-HDACi 1** and **OBHS-HDACi 2** as positive controls for ER binding affinity study. One can see that compound **16c**, which has a similar structure to **OBHS-HDACi 1**, displayed comparable RBA value of 3.68 for ERα, but reduced ERβ binding affinity, resulting in a significantly increased ERα selectivity of 28-fold over ERβ (Table 2, entries 3 vs 26). Similarly, compared with **OBHS-HDACi 2**, although **16i** displayed decreased RBA value for ERα, it also had better ERα selectivity than **OBHS-HDACi 2** (Table 2, entries 9 vs 27).

Table 1
Diels-Alder Reaction of Furan **7** and Dienophiles **12**, **14**–**15**.

Entry	Dienophile		Conv.[a] (%)	Product Yield[b]	
1	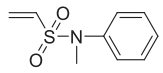	**12a**	97	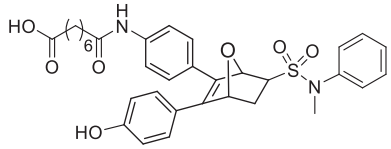	**16a** (94%)
2	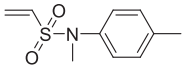	**12b**	99	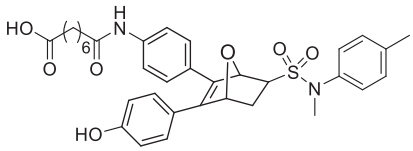	**16b** (95%)
3	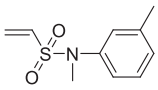	**12c**	98	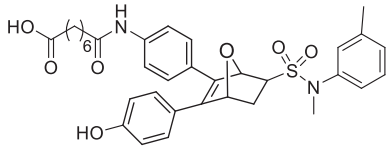	**16c** (96%)
4	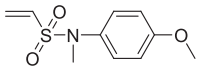	**12d**	97	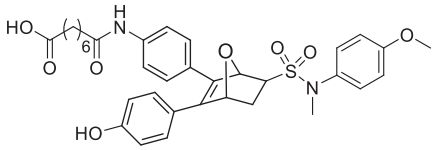	**16d** (94%)
5	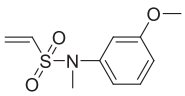	**12e**	97	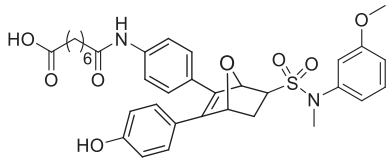	**16e** (95%)
6	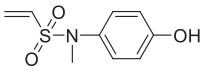	**12f**	96	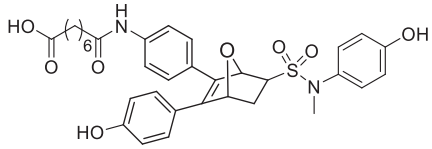	**16f** (91%)
7	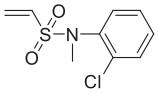	**12g**	95	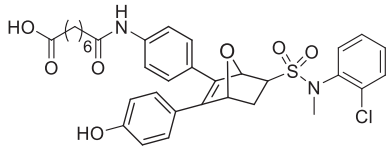	**16g** (93%)
8	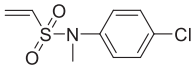	**12h**	93	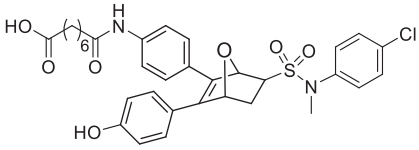	**16h** (89%)
9	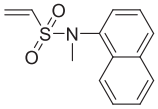	**12i**	97	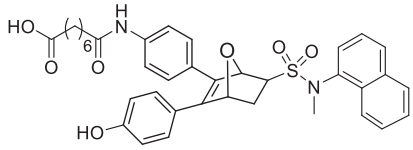	**16i** (95%)
10	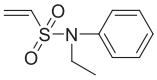	**14a**	96	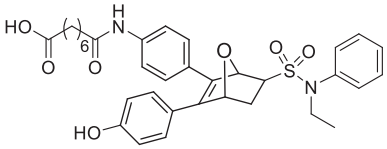	**17a** (94%)

(*continued on next page*)

Table 1 (*continued*)

Entry	Dienophile	Conv.[a] (%)	Product Yield[b]
11	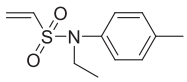 **14b**	98	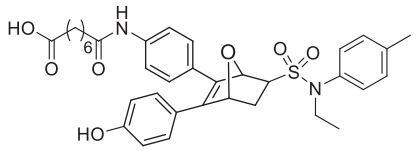 **17b** (96%)
12	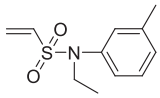 **14c**	96	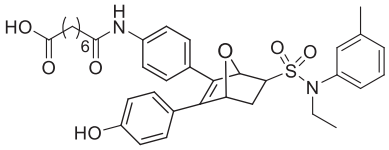 **17c** (94%)
13	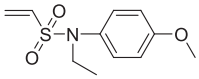 **14d**	94	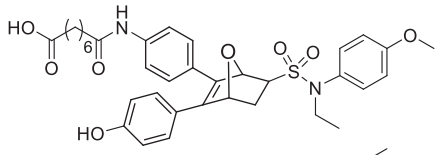 **17d** (91%)
14	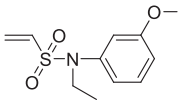 **14e**	96	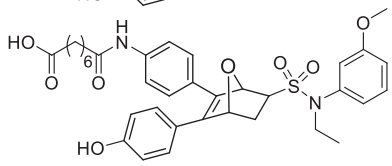 **17e** (94%)
15	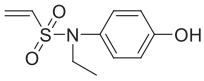 **14f**	97	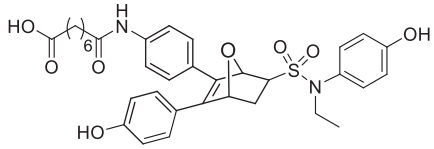 **17f** (93%)
16	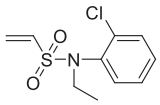 **14g**	90	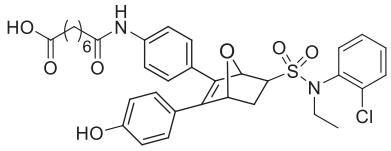 **17g** (87%)
17	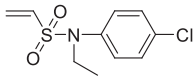 **14h**	92	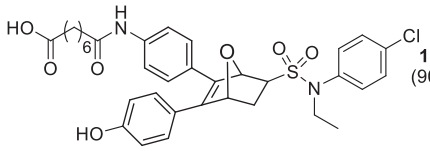 **17h** (90%)
18	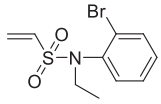 **14i**	91	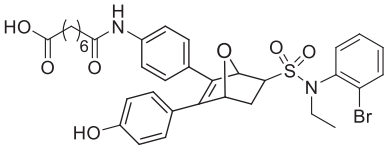 **17i** (89%)
19	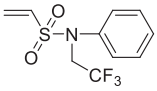 **15a**	99	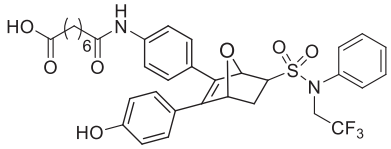 **18a** (97%)
20	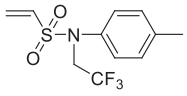 **15b**	97	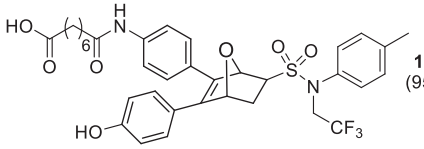 **18b** (95%)

(*continued on next page*)

Table 1 (*continued*)

Entry	Dienophile		Conv.[a] (%)	Product Yield[b]	
21	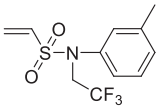	**15c**	98	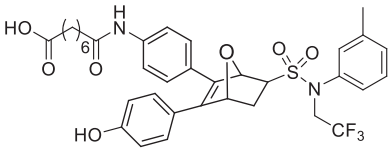	**18c** (94%)
22	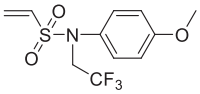	**15d**	97	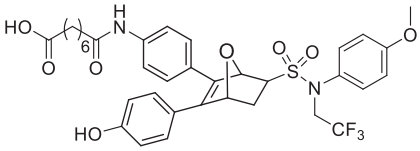	**18d** (95%)
23	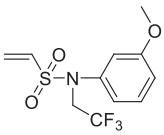	**15e**	99	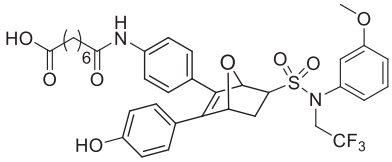	**18e** (96%)
24	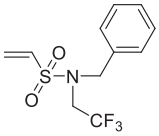	**15f**	96	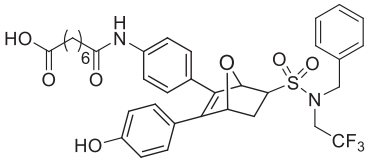	**18f** (94%)

[a]The conversion was calculated accounting for the recovered furan **7**. [b]Isolated yield by column chromatography purification based on furan **7**.

2.3. ER transcriptional activities of OBHSA-HDACi conjugates

ER-responsive luciferase reporter gene assays were used to test the ER transcriptional activities of OBHSA-HDACi conjugates, and the results were summarized in Table 3. We used HEK 293 cells transfected with a widely used 3 × ERE-luciferase reporter to conduct the luciferase assays and analysed the dose–effect curve to get the effect value EC_{50} or antagonism value IC_{50} and efficacy (Eff).

In general, most OBHSA-HDACi conjugates acted as ERα antagonists or ERβ agonists. Almost all the *N*-methyl substituted compounds (**16a-c**, **16e-i**) showed ERα antagonistic activity, except for compound **16d** (Table 3, entry 4) which was a partial agonist of ERα. Moreover, the chloro-substituted compounds **16g** and **16h** were complete antagonists of ERα with the antagonistic IC_{50} up to 5.075 and 5.27 μM, respectively. Additionally, these compounds owned agonistic activity on ERβ, and compound **16a** was capable of agonizing ERβ efficiently with EC_{50} up to 0.12 μM. When *N*-methyl compound was replaced by *N*-ethyl compound, the potency of ERα antagonism was increased (analogues **16a** vs **17a**, Table 3, entries 1 vs 10). After introducing a substituent on the benzene ring of the *N*-ethyl substituted compounds (Table 3, 17a vs **17b-i**), the potency of ERα antagonism was significantly decreased. Interestingly, the chloro-substituted compounds **17g** and **17h** still remained good ERα antagonistic activity. As for the *N*-trifluoroethyl substituted compounds, most of them exhibited relatively weak ERα antagonistic activity, accompanied by the lower affinity for ER. However, they had good agonistic activity on ERβ. Among them, 4-methyl substituted compound **18b** and 4-methoxy substituted compound **18d** performed as full ERβ agonists. In addition, compared with **OBHS**, although the transcription activity of OBHSA-HDACi conjugates decreased when sulfonic acid ester moiety has been changed into sulfonamide group, these conjugates did not display agonistic activity to ERα, thus may avoid potential side effects. After adding a suberic acid to OBHSA, compound **16b** displayed better antagonistic efficacy and lower IC_{50} than the precursor compound **OBHSA-1** (Table 3, entries 2 vs 25).

2.4. Cell viability of OBHSA-HDACi conjugates

All conjugates were tested on hormone-positive (ER+) breast cancer MCF-7 cell lines by MTT method to detect their antiproliferation activity. In order to detect the target selectivity of these conjugates, we used prostate cancer DU-145 cells which were related to abnormal histone deacetylase for comparison. The epithelial kidney cells (VERO cells) were used as normal cells to detect the toxicity of these conjugates. The results of the antiproliferation activity were summarized in Table 4.

Overall, most OHBAS-HDACi conjugates could effectively inhibit the proliferation of breast cancer MCF-7 cells, and would not harm VERO cells, indicating these conjugates have a good safety. Compared with the positive control drug SAHA, although the antiproliferative activity against cancer cells was decreased, the safety was greatly improved. Especially, conjugates **16g**, **16h** and **16i** showed higher antiproliferative activity in MCF-7 cell lines than the approved drug 4-hydroxytamoxifen, accompanying with better safety. However, the substituents on the sulfonamide and the phenyl ring of the benzenesulfonamide had a great influence on the activity. In these three types of conjugates, most *N*-methyl substituted compounds were generally more active than *N*-ethyl or trifluoroethyl substituted compounds. As far as *N*-methyl substituted compounds were concerned, the electron-donating group at the para-position of phenyl sulfonamide moiety offered the bigger contribution to the anti-proliferative activity than that of the meta-position (analogues **16b** vs **16c** and **16d** vs **16e**, Table 4).

Moreover, we observed that compounds **16g** and **16h** had a chlorine substituent compared with **16a** (Table 4, entries 7 and 8 vs 1), resulting in a highly improved anti-proliferative activity. Additionally, the result of **16i** (Table 4, entries 9) indicated that a bigger size substituent was helpful. In the *N*-ethyl substituted compounds, the electron-donating group at the meta-position of benzene ring displayed better activity than that of the para-position (Table 4, analogues **17b** vs **17c** and **17e** vs **17f**), but all of them were weaker than the unsubstituted parent compounds (analogues **17b-f** vs **17a**, Table 3). Furthermore, the results for **17g** and **17i** (Table 4, entries 16 vs 18) suggested that the size of the ortho substituent was important.

Table 2
Relative Binding Affinity (RBA) of OBHSA-HDACi Conjugates for ERα and ERβ.[a]

Entry	Compound		RBA[a] (%)			K_i [b] (nM)		
			ERα	ERβ	α/β ratio	ERα	ERβ	α/β ratio
1	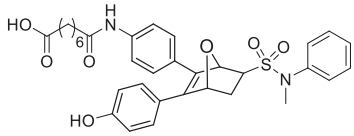	**16a**	13.07 ± 0.23	6.00 ± 0.11	2.17	23.71	56.67	2.39
2	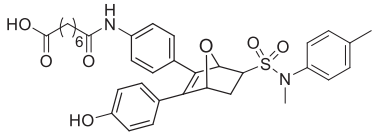	**16b**	0.44 ± 0.01	0.12 ± 0.05	3.67	704.55	2833.33	4.02
3	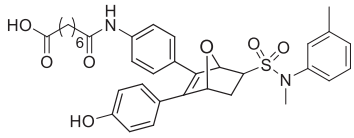	**16c**	3.68 ± 0.77	0.13 ± 0.01	28.31	84.24	2615.38	31.05
4	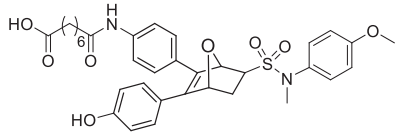	**16d**	5.77 ± 0.15	< 0.01	> 577	53.73	> 5000	> 93.06
5	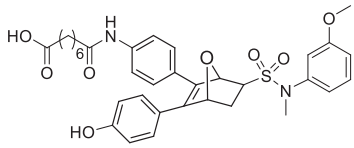	**16e**	1.49 ± 0.01	0.12 ± 0.01	12.42	208.05	2833.33	13.12
6	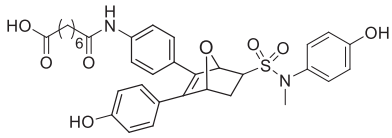	**16f**	2.62 ± 0.41	3.34 ± 0.251	0.78	118.32	101.79	0.86
7	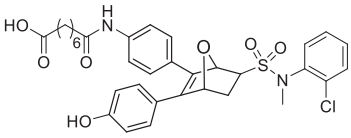	**16g**	11.60 ± 0.32	< 0.01	> 1160	26.72	> 5000	> 187.13
8	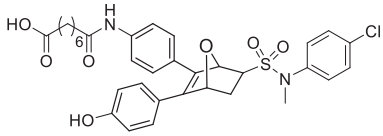	**16h**	1.67 ± 0.47	0.03 ± 0.01	55.67	185.63	> 5000	> 26.94
9	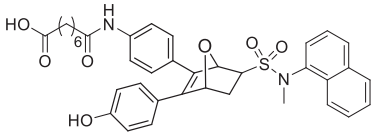	**16i**	0.18 ± 0.20	0.10 ± 0.02	1.80	1722.22	3400.00	1.97
10	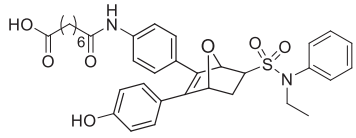	**17a**	1.19 ± 0.23	0.98 ± 0.12	1.21	260.50	346.94	1.33

(*continued on next page*)

Table 2 (*continued*)

Entry	Compound		RBA[a] (%)			K_i [b] (nM)		
			ERα	ERβ	α/β ratio	ERα	ERβ	α/β ratio
11	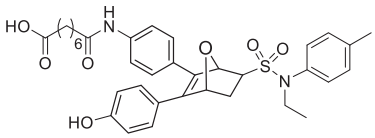	**17b**	0.22 ± 0.01	0.07 ± 0.01	3.14	1409.09	4857.14	3.45
12	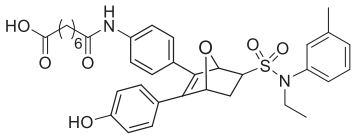	**17c**	0.31 ± 0.01	0.17 ± 0.39	1.82	1000.00	2000.00	2.00
13	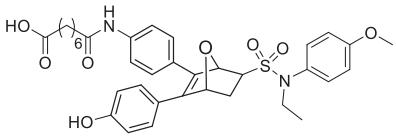	**17d**	0.46 ± 0.03	0.11 ± 0.01	4.18	673.91	3090.91	4.59
14	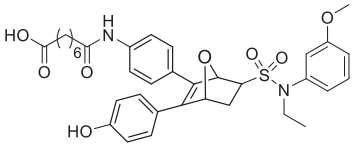	**17e**	2.02 ± 0.30	0.12 ± 0.01	16.83	153.47	2833.33	18.46
15	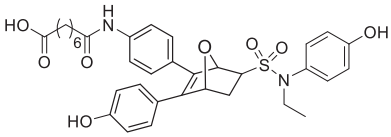	**17f**	1.26 ± 0.33	< 0.01	> 126	246.03	> 5000	> 20.32
16	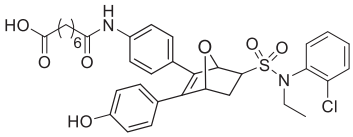	**17g**	0.43 ± 0.01	0.12 ± 0.02	3.58	720.93	2833.33	3.93
17	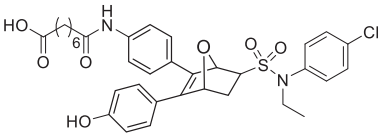	**17h**	0.24 ± 0.04	0.19 ± 0.06	1.26	1291.67	1789.47	1.39
18	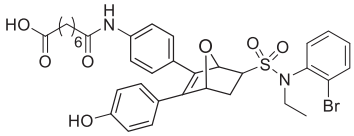	**17i**	0.58 ± 0.12	0.11 ± 0.01	5.27	534.48	3090.90	5.78
19	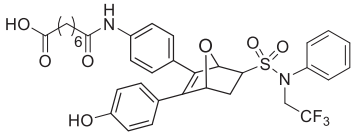	**18a**	0.17 ± 0.01	0.10 ± 0.01	1.70	1823.53	3400.00	1.86
20	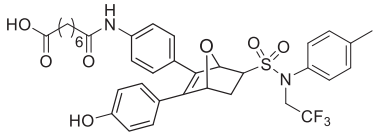	**18b**	0.32 ± 0.03	0.26 ± 0.02	1.23	968.75	1307.69	1.35

(*continued on next page*)

Table 2 (*continued*)

Entry	Compound		RBA[a] (%) ERα	RBA[a] (%) ERβ	α/β ratio	K_i [b] (nM) ERα	K_i [b] (nM) ERβ	α/β ratio
21	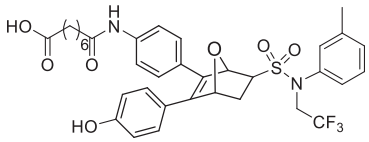	**18c**	0.47 ± 0.02	0.14 ± 0.01	3.36	659.57	2428.57	3.68
22	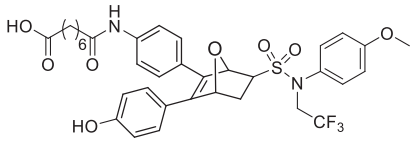	**18d**	0.20 ± 0.05	0.03 ± 0.01	6.67	1550.00	> 5000	> 3.23
23	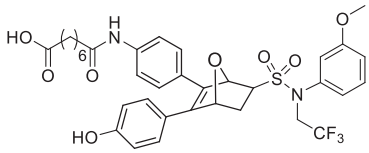	**18e**	0.62 ± 0.18	0.16 ± 0.03	3.88	500.00	2125.00	4.25
24	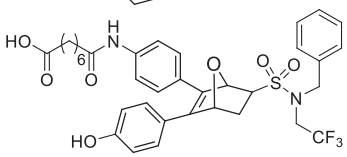	**18f**	0.56 ± 0.02	0.22 ± 0.04	2.55	553.57	1545.45	2.79
25	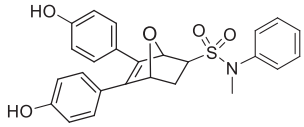	**OBHSA-1**	2.87 ± 0.19	0.75 ± 0.15	3.83	108.01	453.33	4.20
26	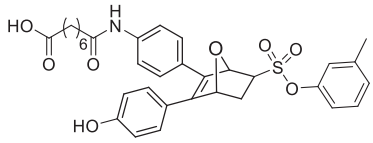	**OBHS -HDACi 1**	3.93 ± 0.82	4.78 ± 0.74	0.82	78.89	71.19	0.90
27	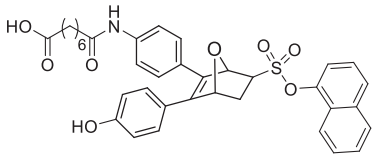	**OBHS -HDACi 2**	1.71 ± 0.08	3.13 ± 0.58	0.55	180.88	108.58	0.60

[a]Relative Binding Affinity (RBA) values are determined by competitive fluorometric binding assays and are expressed as $IC_{50}^{estradiol} / IC_{50}^{compound} \times 100 \pm$ the range (RBA, estradiol = 100%).
[b]K_i values of each conjugate for each receptor were obtained from the RBA values by the formula $K_i = (100/RBA) \times K_d$. The K_d value of estradiol is 3.1 nM for ERα and 3.4 nM for ERβ, respectively. For details, see Experimental Section.

Additionally, all OBHSA-HDACi conjugates are nontoxic to healthy VERO cells, while SAHA and 4OHT showed considerable toxicity. Comparing the activity of conjugates (**16b**,**16d**,**16f-i**,**17a**,**17d** and **17h**) with control drugs SAHA and tamoxifen on VERO, 4OHT had the smallest *in vitro* therapeutic index (IVTI), while our conjugates show greater IVTIs (Table 4). Compared with our previously reported OBHS-HDACi conjugates **OBHS-HDACi 1** and **OBHS-HDACi 2**[41], the antiproliferative activity of OBHSA-HDACi conjugates decreased slightly (Table 4, entries 7 vs 27 and 28), however, these OBHS-HDACi conjugates showed no ERα degradation activity but the OBHSA-HDACi conjugates could potently degrade ERα (See discussion below and Supporting Information on page S42 for details).

2.5. HDAC inhibition activity of OBHSA-HDACi conjugates

In order to verify whether these compounds have dual targeting ability, we selected nine compounds with the best inhibitory ability on MCF-7 cells to test their HDAC inhibition, and some of them showed good inhibitory activity against DU-145.

Class I histone deacetylases (HDAC1, HDAC2, HDAC3 and HDAC8) were related with various solid tumors. They can regulate p53/NF-κB crosstalk in cancer cells.[42] There are also reports that inhibiting class I HDACs can up-regulate acetylation of lysines 9 and 14 of histone H3 in p21Waf1/Cip1 promoter region, thereby up-regulating p21Waf1/Cip1 level and inhibiting cell proliferation.[43] Therefore we first tested acetylation of H3, a major substrate of class I HDACs treated with compounds **16b**, **16d**, **16f-i**, **17a-b**, and **17h** through western blot. As shown

Table 3
Effects of OBHS-HDACi conjugates on the transcriptional activities of estrogen receptor α and β.

		Agonist Mode[a]				Antagonist Mode[b]			
		ERα		ERβ		ERα		ERβ	
entry	Compd.	EC_{50} (μM)	Eff (% E_2)	EC_{50} (μM)	Eff (% E_2)	IC_{50} (μM)	Eff (% E_2)[c]	IC_{50} (μM)	Eff (% E_2)
1	**16a**	–	–	0.12	37 ± 6	–	17 ± 2	–	–
2	**16b**	–	5 ± 1	5.441	57 ± 7	1.254	25 ± 4	–	–
3	**16c**	–	–	1.009	68 ± 22	–	29 ± 6	–	8 ± 1
4	**16d**	–	30 ± 4	–	12 ± 2	–	81 ± 3	0.146	5 ± 2
5	**16e**	–	−4 ± 1	1.005	46 ± 16	5.781	48 ± 1		31 ± 8
6	**16f**	–	−4 ± 1	1.892	64 ± 12	1.396	52 ± 1	–	0.21 ± 4
7	**16g**	–	2 ± 0	38.01	22 ± 9	5.075	14 ± 5	2.11	45 ± 1
8	**16h**	–	1 ± 2	–	–	5.27	28 ± 7	1.876	35 ± 6
9	**16i**	–	−7 ± 1	6.508	53 ± 1	–	75 ± 11	–	–
10	**17a**	–	2 ± 1	0.415	30 ± 3	5.67	−29 ± 6	–	19 ± 2
11	**17b**	–	–	–	11 ± 1	2.08	26 ± 4	0.129	10 ± 1
12	**17c**	–	−1 ± 0	–	10 ± 4	3.68	35 ± 4	45.6	31 ± 3
13	**17d**	–	9 ± 3	0.18	20 ± 2	–	–		14 ± 3
14	**17e**	–	0 ± 1	0.128	62 ± 7	1.106	9 ± 6	–	–
15	**17f**	–	5 ± 2	1.742	57 ± 9	–	107 ± 7	–	15 ± 5
16	**17g**	–	21 ± 1	–	1 ± 0	3.13	5 ± 1	1.174	87 ± 2
17	**17h**	–	–	–	–	2.61	10 ± 2	7.088	78 ± 3
18	**17i**	–	0 ± 3	1.335	43 ± 10	1.87	34 ± 2	–	11 ± 2
19	**18a**	–	−1 ± 2	–	–	5.906	23 ± 4	0.114	68 ± 1
20	**18b**	–	1 ± 0	1.301	80 ± 13	0.043	61 ± 6	–	2 ± 0
21	**18c**	–	15 ± 1	6.12	26 ± 3	6.12	48 ± 1	–	–
22	**18d**	–	–	4.621	72 ± 9	–	–	–	13 ± 1
23	**18e**	–	–	0.122	65 ± 2	–	–		−6 ± 1
24	**18f**	–	–	0.102	47 ± 12	–	–	–	–
25	**OBHSA-1**	–	5 ± 3	–	−1 ± 1	2.32	35 ± 3	1.45	46 ± 2
26	**OBHS**	0.12	53 ± 2	–	3 ± 1	0.042	60 ± 4	0.633	26 ± 3

[a] Luciferase activity was measured in HEK293T cells transfected with 3 × ERE-driven luciferase reporter and expression vectors encoding ERα or ERβ and treated in triplicate with increasing doses (up to 10^{-5} M) of the compounds. EC_{50} and standard deviation (mean ± SD), shown as a percentage of 10^{-8} M 17β-estradiol (E_2), were determined.
[b] IC_{50} and standard deviation (mean ± SD) were determined in the percentage of 10^{-8} M 17β-estradiol(E_2) on ERβ or ERα.
[c] ERs have considerable basal activity in HEK293T cells; compounds with inverse agonist activity are given negative efficacy values. Omitted EC_{50} or IC_{50} values were too high to be determined accurately.

in Fig. 3A, conjugates **16g**, **16i**, **17d** and **17h** can significantly increase the acetylation of H3, which meant that these compounds could inhibit class I HDACs.

Furthermore, HDAC6 has been reported to play an important role in the metastasis and invasion of breast cancer, which deacetylates α-tubulin and increases cell motility.[44] Then the effect of above OBHSA-HDACi conjugates on acetylation of α-tubulin were also tested. As Fig. 3B shown, conjugates **16d**, **16g**, **16h** and **16i** can significantly increase the acetylation of α-tubulin. In general, most of these compounds showed a certain inhibitory ability to HDACs, among them, compounds **16g** and **16i** can inhibit the activity of HDAC6 and class I HDACs simultaneously.

As a final test, the direct inhibitory activity of OBHSA-HDACi conjugates **16g** and **16i** with significant antiproliferative effects on MCF-7 cell lines were assayed for HDAC6 and HDAC8, which have been implicated critical for invasion in breast cancer,[45] and showed good inhibitory activity with IC_{50} values ranged from 1.32 to 4.53 μM, and the results are shown in Table 5.

2.6. The effect of the conjugates on the degradation of ERα

Next, we investigated the ability to down-regulate ERα of OBHSA-HDACi and the results showed in Fig. 4. As the Fig. 4A shown, **16b**, **16d**, **16f-h**, **17a**, **17d**, **17h** had little ERα down-regulating activity, while the conjugate **16i** exhibited strong ERα down-regulating ability. After treating with conjugate **16i**, the expression of ERα in MCF-7 cells decreased by 78% compared with untreated group.

Furthermore, we investigated the possible mechanism of down-regulating ERα by conjugate **16i**. ERα protein level was reduced when treated with 20 μM **16i** alone, but in the presence of 10 μM MG-132, a proteasome inhibitor, ERα protein level significantly increased compared to that in the absence of MG-132 (Fig. 4B), which confirmed that the degradation of ERα was mediated through proteasome-mediated process.

2.7. Computer modeling

As mentioned above, both conjugates **16g** and **16i** showed significant antiproliferative activity on MCF-7 cell lines, in which only conjugate **16i** could also degrade ERα protein. We suspect that this may be related to the different interaction of conjugates with ERα protein, thus, molecular docking was performed to analyze the interactions between the conjugates **16g** and **16i** and ERα (PDB: 5KD9).

As shown in Fig. 5A, we observed that the phenol group of conjugate **16g** could form a hydrogen bond with Thr 347 (2.71 Å) and the suberic acid side chain could generate strong steric clashes with helix 11 by engaging in hydrogen bonding with Val 534 (2.83 Å) and indirectly regulate helix 12, which was crucial for the antagonism (See Supporting Information for the 2D images of compounds **16g** and **16i** binding to ERα). In addition, the chlorine substituent could form a halogen bond with Met 343. All of the interactions resulted in a significant enhancement of the binding ability to the protein, thus conjugate **16g** displayed good anti-proliferative activity against MCF-7 cells. However, in Fig. 5B, the ligand could only form a hydrogen bond with Thr 347 (2.71 Å), which explained **16i** had moderate binding affinity. More importantly, because of the π-π stacking interaction formed by naphthyl substituent and Phe 404, the suberic acid side chain flipped toward helix 3 and close to Asp 351, which is closely related to protein degradation. Additionally, conjugate **16i** could induce a rotation of helix 11C terminus by shifting His 524 and Leu525, and further altering the interface between helix 11 and helix 12, which finally cause protein degradation.

Table 4
The antiproliferative activity of OBHSA-HDACi conjugate (IC_{50}, μM).[a]

Entry	Compound	MCF-7	DU-145	VERO	IVTI[c]
1	**16a**	63.8 ± 1.33	>100[b]	>100	>1.5
2	**16b**	23.2 ± 1.43	>100	>100	>4.3
3	**16c**	30.2 ± 3.65	>100	>100	>3.3
4	**16d**	24.8 ± 1.87	67.1 ± 0.63	>100	>4.0
5	**16e**	39.4 ± 2.32	62.2 ± 4.63	>100	>2.5
6	**16f**	20.8 ± 1.14	>100	>100	>4.8
7	**16g**	12.8 ± 0.16	73.5 ± 1.01	>100	>7.8
8	**16h**	13.7 ± 1.15	72.1 ± 0.59	>100	>7.2
9	**16i**	14.0 ± 1.71	70.9 ± 0.56	>100	>7.1
10	**17a**	19.1 ± 1.77	>100	>100	>5.2
11	**17b**	42.3 ± 7.02	53.5 ± 1.99	>100	>2.3
12	**17c**	31.8 ± 2.21	65.6 ± 6.76	>100	>3.1
13	**17d**	20.3 ± 1.56	24.4 ± 3.07	>100	>4.9
14	**17e**	37.4 ± 1.79	71.1 ± 1.24	>100	>2.6
15	**17f**	46.6 ± 3.86	>100	>100	>2.1
16	**17g**	33.3 ± 1.56	>100	>100	>3.0
17	**17h**	22.1 ± 2.23	42.1 ± 4.49	>100	>4.5
18	**17i**	>100	95.3 ± 2.02	>100	NT[d]
19	**18a**	62.1 ± 3.81	68.5 ± 0.93	>100	>1.6
20	**18b**	96.0 ± 0.83	74.7 ± 0.52	>100	>1.0
21	**18c**	69.5 ± 0.47	49.8 ± 2.92	>100	>1.4
22	**18d**	>100	66.5 ± 0.83	>100	NT
23	**18e**	72.0 ± 0.14	72.0 ± 0.14	>100	>1.3
24	**18f**	>100	69.9 ± 1.07	>100	NT
25	**SAHA**	2.50 ± 0.33	1.2 ± 0.07	4.1 ± 0.19	1.6
26	**4OTH**	15.6 ± 1.77	15.3 ± 4.42	15.1 ± 5.21	1.0
27	**OBHS-HDACi 1**	5.8 ± 0.85	66.3 ± 4.62	>100	>17.2
28	**OBHS-HDACi 2**	8.12 ± 0.38	59.6 ± 0.95	>100	>12.3

[a] IC_{50} values are an average of at least three independent experiments ± standard deviation (mean ± SD).
[b] IC_{50} not determinable up to highest concentrations tested.
[c] IVTI = IC_{50}(VERO)/IC_{50}(MCF-7).
[d] NT = inhibition not detectable.

3. Conclusion

The occurrence of breast cancer is related to many factors,[33] involving multiple signal pathways. Among them, the ERα-mediated signal pathway plays an important role in the development of breast cancer.[46] Therefore, ERα is an important target for the treatment of breast cancer. However, most clinically used ER ligands are ERα partial antagonists with serious side effects, and SERDs are possible to overcome these problems by directly degrading ERα protein to shut down ERα signaling pathways. While dozens of ERα degradants have been reported and entered clinical trials, no ER degradants have been approved for marketing. Therefore, the development of novel, efficient and safe degradants is urgently needed. In this study, we designed and synthesized a series of novel OBHSA-HDACi conjugates that contained SERD and HDACi units and investigated their antiproliferative activity and mechanism of action. As a result, conjugate **16i** with *N*-methyl and naphthyl groups exhibited excellent antiproliferative activity against MCF-7 cell lines and ERα degradation activity, which also exhibited potent inhibitory ability to HDACs. Molecular docking analysis indicated the interaction of naphthyl and suberic acid side of conjugate **16i** with ERα may be the main reasons for the degradation of ERα protein. In summary, the OBHSA-HDACi conjugates may provide possibilities for discovery of novel SERDs or PROTAC-like compounds for breast cancer treatment.

Table 5
IC_{50} values of conjugates **16g** and **16i** for inhibition of HDAC8 and HDAC6.[a]

Entry	Compound	HDAC8 (μM)	HDAC6 (μM)
1	**16g**	3.35	4.53
2	**16i**	3.94	1.32
3	**Vorinostat (SAHA)**	0.01	0.014

[a] Values are the means of a minimum of three experiments.

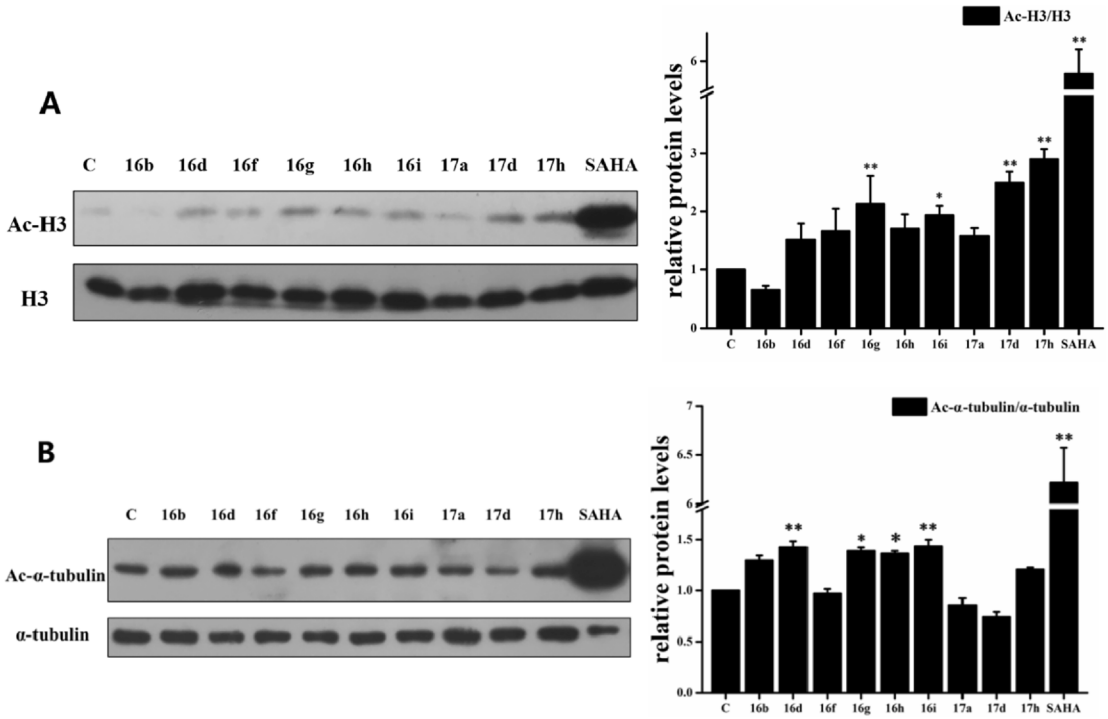

Fig. 3. (A) Western blot assay of Ac-H3 in DU-145 cells treated with different conjugates at 20 μM for 24 h. (B) Western blot assay of Ac-α-tubulin in DU-145 cells treated with different conjugates at 20 μM for 24 h. Histograms were shown as the mean ± S.D. of at least 3 independent experiments. The western blots shown are representative of at least three independent experiments. * $p < 0.05$, ** $p < 0.01$ compared to control.

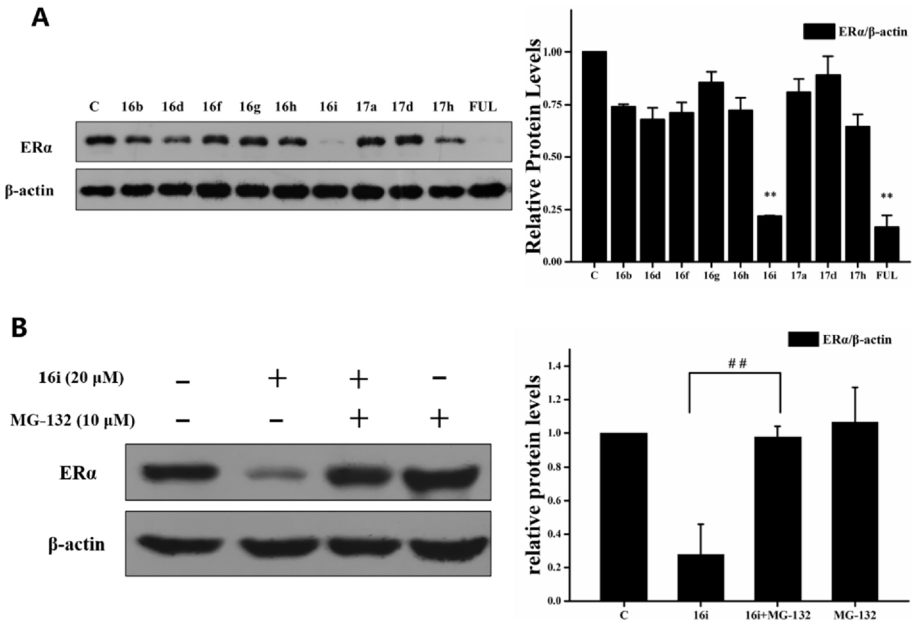

Fig. 4. (A) Western blot assay of ERα in MCF-7 cells treated with different conjugates at 20 μM for 24 h. (B) Western blot assay of ERα in MCF-7 cells treated with compound **16i** and protostome inhibitor MG-132 for 24 h. Histograms were shown as the mean ± S.D. of at least 3 independent experiments. The western blots shown are representative of at least three independent experiments. **p < 0.01 compared to control; ##p < 0.01 compared to 16i-treated group.

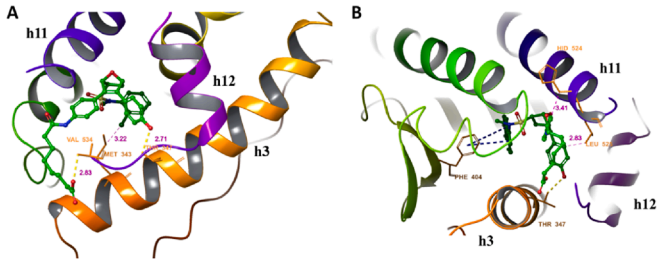

Fig. 5. Computer modeling of OBHS-HDACi conjugates **16g** (A) and **16i** (B) bound to ERα (PDB: 5KD9).

4. Experimental section

4.1. Materials and methods

All chemicals and solvents were purchased from commercial sources and were used without further purification. Tetrahydrofuran (THF) was dried over Na and distilled prior to use. ^{1}H NMR and ^{13}C NMR spectra were recorded on a Bruker Biospin AV400 (400 MHz) instrument. Chemical shifts are reported in ppm (parts per million) and are referenced to either tetramethylsilane or the solvent. A purity of >95% for all the final compounds was determined with HPLC (Agilent Technologies) and UV detection at 254 nm.

4.2. General procedures for Diels-Alder reaction (*16a-i, 17a-i* and *18a-f*)

Furan **7** (0.5 mmol) and dienophiles **12**, **14**–**15** (0.6 mmol) were distilled THF (2 mL), and the reaction mixture was stirred at 90 °C for 12 h. The crude product was purified by silica gel column chromatography (Dichlormethane-MeOH, 60 : 1 ~ 30 : 1)

8-(4-(-6-(*N*-(4-Hydroxyphenyl)-*N*-methylsulfamoyl)-3-(4-hydroxyphenyl)-7-oxabicyclo [2.2.1] hept-2-en-2-yl)phenylamino)-8-oxooctanoic acid (16a). Pale yellow solid, 94% yield, m.p. 113–115 °C; ^{1}H NMR(400 MHz, Acetone-d_6) δ 9.14(s, 1H, —CONH—), 7.49(t, J = 8.8 Hz, 2H), 7.29(t, J = 8.4 Hz, 2H), 7.20(t, J = 8.4 Hz, 2H), 7.12(d, J = 8.0 Hz, 2H), 7.10(d, J = 8.4 Hz, 1H), 7.04(d, J = 8.0 Hz, 1H), 7.02(d, J = 8.0 Hz, 1H), 6.69(d, J = 8.8 Hz, 1H), 6.60(d, J = 8.8 Hz, 1H), 5.35(s, 1H), 5.18(t, J = 3.2 Hz, 1H), 3.49(m, 1H), 3.24(m, 3H), 2.23(m, 2H), 2.13(t, J = 6.4 Hz, 2H), 1.92(m, 1H), 1.83(m, 1H), 1.54(m, 2H), 1.45(t, J = 6.4 Hz, 2H), 1.23(m, 4H). ^{13}C NMR(100 MHz, Acetone-d_6) δ 174.83, 172.18, 158.42, 143.12, 141.56, 140.00, 139.56, 137.93, 129.98, 129.83, 129.66, 128.76, 128.46, 127.71, 127.41, 127.35, 124.86, 124.26, 120.10, 119.93, 116.53, 116.37, 85.20, 83.59, 61.60, 39.21, 39.17, 37.65, 34.16, 31.32, 32.13, 26.11, 25.52; HRMS(ESI) calcd for $C_{33}H_{35}N_2O_7S$ [M - H]$^-$, 603.2165; found 603.2170.

8-(4-(3-(4-Hydroxyphenyl)-6-(*N*-methyl-*N*-(p-tolyl)sulfamoyl)-7-oxabicyclo [2.2.1] hept-2-en-2-yl)phenylamino)-8-oxooctanoic acid (16b). Pale yellow solid, 95% yield, m.p. 114–117 °C; ^{1}H NMR (400 MHz, Acetone-d_6) δ 9.24(s, 1H, —CONH—), 7.63(d, J = 8.0 Hz, 2H), 7.30(d, J = 8.8 Hz, 1H), 7.29(d, J = 8.8 Hz, 1H), 7.26(d, J = 8.8 Hz, 1H), 7.23(d, J = 8.4 Hz, 1H), 7.18(d, J = 8.4 Hz, 2H), 7.14(d, J = 8.0 Hz, 2H), 6.81(d, J = 8.4 Hz, 1H), 6.80(d, J = 8.8 Hz, 1H), 5.47(s, 1H), 5.32 (s, 1H), 3.59(m, 1H), 3.35(s, 3H), 2.38(t, J = 7.2 Hz, 2H), 2.31(m, 2H), 2.29(s, 3H), 2.13(m, 1H), 2.06(m, 1H), 1.68(t, J = 6.4 Hz, 2H), 1.59(t, J = 7.2 Hz, 2H), 1.37(m, 4H). ^{13}C NMR(100 MHz, Acetone-d_6) δ 174.98, 172.42, 158.38, 143.18, 141.57, 140.48, 137.97, 137.52, 130.39, 130.01, 129.66, 128.80, 128.45, 127.38, 127.30, 124.93, 124.31, 120.27, 120.12, 116.59, 116.44, 85.26, 83.58, 61.49, 39.33, 37.73, 34.21, 31.36, 31.17, 29.66, 26.15, 25.54, 21.01; HRMS(ESI) calcd for $C_{34}H_{37}N_2O_7S$ [M - H]$^-$, 617.2321; found 617.2327.

8-(4-(3-(4-Hydroxyphenyl)-6-(*N*-methyl-*N*-(m-tolyl)sulfamoyl)-7oxabicyclo [2.2.1] hept-2-en-2-yl)phenylamino)-8-oxooctanoic acid (16c). Pale yellow solid, 96% yield, m.p. 120–123 °C; ^{1}H NMR(400 MHz, Acetone-d_6) δ 9.24(s, 1H, —CONH—), 7.63(d, J = 8.4 Hz, 1H), 7.60(d, J = 8.8 Hz, 1H), 7.24(d, J = 8.0 Hz, 2H), 7.22(m, 3H), 7.20(d, J = 8.8 Hz, 1H), 7.18(d, J = 8.4 Hz, 1H), 7.08(d, J = 8.8 Hz, 1H), 6.81(d, J = 8.8 Hz, 1H), 6.80(d, J = 8.8 Hz, 1H), 5.50(s, 1H), 5.32(s, 1H), 3.61(m, 1H), 3.36(s, 3H), 2.37(t, J = 6.8 Hz, 2H), 2.32(m, 2H), 2.28(s, 3H), 2.16 (m, 1H), 2.06(m, 1H), 1.68(m, 2H), 1.59(t, J = 6.4 Hz, 2H), 1.37(m, 4H). ^{13}C NMR(100 MHz, Acetone-d_6) δ 174.93, 172.34, 158.45, 143.17, 143.04, 141.62, 139.69, 137.95, 130.00, 129.65, 129.62, 128.78, 128.44, 127.99, 127.91, 124.94, 124.42, 124.34, 120.24, 120.08, 116.61, 116.42, 85.24, 83.57, 61.44, 39.26, 37.71, 34.19, 31.35, 31.16, 26.13, 25.53, 21.40, 20.58; HRMS(ESI) calcd for $C_{34}H_{37}N_2O_7S$ [M - H]$^-$,

617.2321; found 617.2327.

8-(4-(3-(4-Hydroxyphenyl)-6-(*N*-(4-methoxyphenyl)-*N*-methylsulfamoyl)-7-oxabicyclo [2.2.1] hept-2-en-2-yl)phenylamino)-8-oxooctanoic acid (16d). Pale yellow solid, 94% yield, m.p. 107–109 °C; ^{1}H NMR(400 MHz, Acetone-d_6) δ 9.23(s, 1H, —CONH—), 7.64(d, J = 8.8 Hz, 1H), 7.60(d, J = 8.8 Hz, 1H), 7.30(d, J = 8.4 Hz, 2H), 7.26(d, J = 8.4 Hz, 2H), 7.20(d, J = 8.4 Hz, 2H), 6.84(d, J = 8.8 Hz, 2H), 6.82(d, J = 8.8 Hz, 1H), 6.80(d, J = 8.4 Hz, 1H), 5.49(s, 1H), 5.33(t, J = 2.8 Hz, 1H), 3.78(s, 3H), 3.53(m, 1H), 3.33(s, 3H), 2.37(t, J = 7.2 Hz, 2H), 2.29(t, J = 7.2 Hz, 2H), 2.16(m, 1H), 2.06(m, 1H), 1.68(t, J = 6.8 Hz, 2H), 1.60(t, J = 7.2 Hz, 2H), 1.37(m, 4H). ^{13}C NMR(100 MHz, Acetone-d_6) δ 174.87, 172.23, 159.50, 158.44, 143.08, 141.56, 140.04, 139.65. 138.01, 135.59, 130.07, 129.62, 129.22, 128.88, 128.43, 124.96, 124.35, 120.28, 120.07, 116.58, 116.41, 114.92, 85.31, 83.58, 61.25, 55.78, 39.61, 37.71, 34.17, 31.38, 31.20, 26.12, 25.52, 20.55; HRMS(ESI) calcd for $C_{34}H_{37}N_2O_8S$ [M - H]$^-$, 633.2271; found 633.2276.

8-(4-(3-(4-Hydroxyphenyl)-6-(*N*-(3-methoxyphenyl)-*N*-methylsulfamoyl)-7-oxabicyclo [2.2.1] hept-2-en-2-yl)phenylamino)-8-oxooctanoic acid (16e). Pale yellow solid, 95% yield, m.p. 105–107 °C; ^{1}H NMR(400 MHz, Acetone-d_6) δ 9.28(s, 1H, —CONH—), 7.62(d, J = 8.4 Hz, 2H), 7.23(d, J = 8.0 Hz, 2H), 7.20(d, J = 8.0 Hz, 2H), 7.18(d, J = 8.4 Hz, 1H), 7.03(m, 2H), 6.82(d, J = 8.0 Hz, 1H), 6.80(d, J = 8.8 Hz, 2H), 5.49(s, 1H), 5.33(s, 1H), 3.76(s, 3H), 3.60(m, 1H), 3.38(s, 3H), 2.39(t, J = 6.8 Hz, 2H), 2.29(t, J = 6.8 Hz, 2H), 2.15(m, 1H), 2.05(m, 1H), 1.68(t, J = 6.0 Hz, 2H), 1.59(t, J = 6.0 Hz, 2H), 1.38(m, 4H). ^{13}C NMR(100 MHz, Acetone-d_6) δ 174.97, 172.40, 160.98, 158.38, 144.22, 143.22, 141.63, 139.56, 137.93, 130.47, 129.92, 129.70, 128.71, 128.49, 124.90, 124.28, 120.25, 119.00, 116.58, 116.43, 113.20, 113.15, 85.20, 83.66, 61.69, 55.73, 39.14, 37.72, 34.19, 31.37, 31.17, 26.13, 25.53, 20.58; HRMS(ESI) calcd for $C_{34}H_{37}N_2O_8S$ [M - H]$^-$, 633.2271; found 633.2276.

8-(4-(3-(4-Hydroxyphenyl)-6-(*N*-methyl-*N*-phenylsulfamoyl)-7-oxabicyclo [2.2.1] hept-2-en-2-yl)phenylamino)-8-oxooctanoic acid (16f). Pale yellow solid, 91% yield, m.p. 122–124 °C; ^{1}H NMR(400 MHz, Acetone-d_6) δ 9.14(s, 1H, —CONH—), 7.46(d, J = 8.8 Hz, 2H), 7.13(d, J = 8.8 Hz, 2H), 7.07(t, J = 8.0 Hz, 4H), 6.70(d, J = 8.0 Hz, 2H), 6.65(d, J = 8.8 Hz, 2H), 5.39(s, 1H), 5.19(s, 1H), 3.41(m, 1H), 3.17(s, 3H), 2.26(t, J = 7.2 Hz, 2H), 2.15(t, J = 7.6 Hz, 2H), 2.03(m, 1H), 1.91 (m, 1H), 1.55(t, J = 6.0 Hz, 2H), 1.45(t, J = 7.2 Hz, 2H), 1.23(m, 4H). ^{13}C NMR(100 MHz, Acetone-d_6) δ 175.13, 172.57, 158.47, 157.40, 141.50, 139.92, 139.69, 134.51, 130.08, 129.44, 129.05, 128.44, 124.28, 120.17, 116.61, 116.38, 85.30, 83.60, 61.10, 39.74, 37.72, 34.23, 31.40, 30.72, 29.65, 26.16, 25.53; HRMS(ESI) calcd for $C_{33}H_{35}N_2O_8S$ [M - H]$^-$, 619.2115; found 633.2120.

8-(4-(-6-(*N*-(2-Chlorophenyl)-*N*-methylsulfamoyl)-3-(4-hydroxyphenyl)-7-oxabicyclo [2.2.1] hept-2-en-2-yl)phenylamino)-8-oxooctanoic acid (16g). Pale yellow solid, 93% yield, m.p. 135–138 °C; ^{1}H NMR(400 MHz, Acetone-d_6) δ 9.31(s, 1H, —CONH—), 7.64(t, J = 8.0 Hz, 2H), 7.54(m, 1H), 7.48(m, 1H), 7.35(m, 2H), 7.30(d, J = 8.0 Hz, 1H), 7.28(d, J = 8.0 Hz, 1H), 7.24(d, J = 8.4 Hz, 1H), 7.22(d, J = 8.0 Hz, 1H), 6.84(d, J = 8.0 Hz, 1H), 6.82(d, J = 8.0 Hz, 1H), 5.60(s, 1H), 5.40 (s, 1H), 3.74(m, 1H), 3.29(s, 3H), 2.39(t, J = 7.6 Hz, 3H), 2.29(t, J = 7.6 Hz, 2H), 2.24(m, 1H), 1.69(t, J = 7.2 Hz, 2H), 1.60(t, J = 7.2 Hz, 2H), 1.36(m, 4H). ^{13}C NMR(100 MHz, Acetone-d_6) δ 175.10, 172.56, 158.43, 143.39, 141.78, 140.05, 139.98, 139.81, 134.97, 132.73, 131.36, 130.58, 130.13, 129.68, 128.90, 128.46, 124.95, 124.27, 120.31, 120.19, 116.64, 116.49, 85.44, 83.67, 63.51, 39.38, 37.74, 34.25, 31.74, 29.67, 26.17, 25.55, 20.68; HRMS(ESI) calcd for $C_{33}H_{34}ClN_2O_7S$ [M - H]$^-$, 637.1776; found 637.1781.

8-(4-(-6-(*N*-(4-chlorophenyl)-*N*-methylsulfamoyl)-3-(4-hydroxyphenyl)-7-oxabicyclo [2.2.1] hept-2-en-2-yl)phenylamino)-8-oxooctanoic acid (16h). Pale yellow solid, 89% yield, m.p. 141–143 °C; ^{1}H NMR(400 MHz, Acetone-d_6) δ 9.28(s, 1H, —CONH—), 7.63(d, J = 8.0 Hz, 1H), 7.60(d, J = 8.8 Hz, 1H), 7.46(d, J = 8.0 Hz, 1H), 7.45(d, J = 8.0 Hz, 1H), 7.36(d, J = 8.8 Hz, 2H), 7.26(d, J = 8.0 Hz, 1H), 7.24(d, J = 8.0 Hz, 1H), 7.19(d, J = 8.4 Hz, 1H), 7.18(d, J = 8.0 Hz, 1H), 6.81(d, J = 8.8 Hz, 1H), 6.80(d, J = 8.8 Hz, 1H), 5.50(s, 1H), 5.34(t, J = 2.8 Hz, 1H), 3.65(m, 1H), 3.38(s, 3H), 2.38(t, J = 7.2 Hz, 2H), 2.29(t, J = 7.2 Hz, 2H), 2.07(m, 2H), 1.68(m, 2H), 1.60(t, J = 6.4 Hz, 2H), 1.37(m, 4H). ^{13}C NMR(100 MHz, Acetone-d_6) δ 175.10, 172.50, 158.50, 143.18, 141.96, 141.58, 139.49. 137.80, 132.71, 129.99, 129.82, 129.68, 128.87, 128.83, 128.80, 128.84, 124.80, 124.20, 120.32, 120.14, 116.61, 116.45, 85.24, 83.57, 61.78, 39.14, 37.73, 34.23, 31.36, 31.15, 26.15, 25.54, 20.66; HRMS(ESI) calcd for $C_{33}H_{34}ClN_2O_7S$ [M - H]$^-$, 637.1776; found 637.1781.

8-(4-(3-(4-hydroxyphenyl)-6-(*N*-methyl-*N*-(naphthalen-1-yl) sulfamoyl)-7-oxabicyclo [2.2.1] hept-2-en-2-yl)phenylamino)-8-oxooctanoic acid (16i). Pale yellow solid, 95% yield, m.p. 115–118 °C; ^{1}H NMR(400 MHz, Acetone-d_6) δ 9.27(s, 1H, —CONH—), 8.74(s, 1H), 8.22(t, J = 8.8 Hz, 1H), 7.92(t, J = 8.4 Hz, 2H), 7.67(d, J = 8.0 Hz, 1H), 7.63(d, J = 8.4 Hz, 2H), 7.54(d, J = 8.8 Hz, 2H), 7.45(m, 1H), 7.29(t, J = 8.8 Hz, 2H), 7.23(d, J = 8.4 Hz, 2H), 6.833(d, J = 8.4 Hz, 2H), 5.59(s, 1H), 5.44(d, J = 3.6 Hz, 1H), 3.86(m, 1H), 3.43(s, 3H), 2.46(m, 1H), 2.38(t, J = 7.2 Hz, 2H), 2.29(t, J = 7.2 Hz, 2H), 2.23(m, 1H), 1.69(t, J = 6.4 Hz, 2H), 1.61(t, J = 6.4 Hz, 2H), 1.37(m, 4H). ^{13}C NMR(100 MHz, Acetone-d_6) δ 174.99, 172.33, 158.46, 143.29, 141.71, 140.06, 139.81, 135.72, 132.93, 130.17, 129.99, 129.68, 128.46, 127.65, 127.36, 124.81, 120.35, 120.12, 116.64, 116.49, 85.58, 83.77, 62.59, 40.80, 37.72, 34.22, 29.67, 29.59, 26.15, 25.55, 20.63; HRMS(ESI) calcd for $C_{37}H_{37}N_2O_7S$ [M - H]$^-$, 653.2323; found 653.2327.

8-(4-(6-(*N*-Ethyl-*N*-phenylsulfamoyl)-3-(4-hydroxyphenyl)-7-oxabicyclo [2.2.1] -hept-2-en-2-yl)phenylamino)-8-oxooctanoic acid (17a). Pale yellow solid, 94% yield, m.p. 131–133 °C; ^{1}H NMR (400 MHz, Acetone-d_6) δ 9.09(s, 1H, —CONH—), 7.52(d, J = 8.8 Hz, 1H), 7.49(d, J = 8.8 Hz, 1H), 7.29(d, J = 8.8 Hz, 1H), 7.22(d, J = 8.0 Hz, 3H), 7.17(m, 1H), 7.13(d, J = 8.4 Hz, 2H), 7.07(d, J = 8.0 Hz, 1H), 7.06 (d, J = 8.0 Hz, 1H), 6.70(d, J = 8.8 Hz, 1H), 6.66(d, J = 8.8 Hz, 1H), 5.36 (s, 1H), 5.20(s, 1H), 3.71(m, 2H), 3.37(m, 1H), 2.24(t, J = 7.6 Hz, 2H), 2.15(t, J = 7.2 Hz, 2H), 2.05(m, 1H), 1.92(m, 1H), 1.55(t, J = 7.2 Hz, 2H), 1.46(t, J = 7.2 Hz, 2H), 1.24(m, 4H), 0.89(t, J = 7.2 Hz, 3H). ^{13}C NMR(100 MHz, Acetone-d_6) δ 174.30, 171.79, 157.71, 142.21, 140.54, 139.29, 139.05, 138.78, 136.99, 129.21, 129.18, 129.00, 128.66, 127.94, 127.55, 127.44, 123.85, 123.17, 119.38, 119.19, 115.71, 115.52, 84.37, 82.66, 61.41, 46.21, 36.77, 33.39, 30.42, 28.73, 25.25, 24.63, 19.82, 14.01; HRMS(ESI) calcd for $C_{34}H_{37}N_2O_7S$ [M - H]$^-$, 617.2321; found 631.2327.

8-(4-(-6-(*N*-Ethyl-*N*-(p-tolyl)sulfamoyl)-3-(4-hydroxyphenyl)-7-oxabicyclo [2.2.1] hept-2-en-2-yl)pheny)amino)-8-oxooctanoic acid (17b). Pale yellow solid, 96% yield, m.p. 137–139 °C; ^{1}H NMR (400 MHz, Acetone-d_6) δ 9.09(s, 1H, —CONH—), 7.49(d, J = 8.8 Hz, 1H), 7.46(d, J = 8.4 Hz, 1H), 7.10(d, J = 8.4 Hz, 2H), 7.07(d, J = 8.0 Hz, 2H), 7.05(d, J = 8.0 Hz, 2H), 7.00(d, J = 8.0 Hz, 2H), 6.70(d, J = 8.4 Hz, 1H), 6.64(d, J = 8.8 Hz, 1H), 5.35(s, 1H), 5.19(s, 1H), 3.66(m, 2H), 3.37 (m, 1H), 2.23(t, J = 7.2 Hz, 2H), 2.16(s, 3H), 2.14(m, 2H), 2.05(m, 1H), 1.91(m, 1H), 1.54(t, J = 7.2 Hz, 2H), 1.45(t, J = 6.8 Hz, 2H), 1.23(m, 4H), 0.88(t, J = 6.8 Hz, 3H). ^{13}C NMR(100 MHz, Acetone-d_6) δ 174.94, 172.32, 158.51, 143.13, 141.58, 140.19, 139.78, 138.04, 130.68, 130.15, 129.65, 129.47, 129.15, 128.93, 128.35, 127.03, 125.01, 124.28, 120.24, 120.06, 116.64, 116.42, 85.25, 83.57, 62.24, 47.16, 37.71, 34.19, 31.35, 31.10, 26.13, 25.53, 21.32, 20.59, 14.98; HRMS (ESI) calcd for $C_{35}H_{39}N_2O_7S$ [M - H]$^-$, 647.2478; found 631.2483.

8-(4-(6-(*N*-Ethyl-*N*-(m-tolyl)sulfamoyl)-3-(4-hydroxyphenyl)-7-oxabicyclo [2.2.1] hept-2-en-2-yl)phenylamino)-8-oxooctanoic aid (17c). Pale yellow solid, 94% yield, m.p. 134–137 °C; ^{1}H NMR(400 MHz, Acetone-d_6) δ 9.23(s, 1H, —CONH—), 7.65(d, J = 8.8 Hz, 1H), 7.60(d, J = 8.8 Hz, 1H), 7.29(s, 1H), 7.27(d, J = 8.8 Hz, 1H), 7.25(d, J = 8.0 Hz, 1H), 7.22(m, 2H), 7.16(d, J = 8.4 Hz, 2H), 7.12(d, J = 8.8 Hz, 1H), 6.85(d, J = 8.4 Hz, 1H), 6.80(d, J = 8.8 Hz, 1H), 5.52(s, 1H), 5.34 (s, 1H), 3.81(m, 2H), 3.52(m, 1H), 2.37(m, 2H), 2.29(m, 2H), 2.27(s, 3H), 2.20(m, 1H), 2.06(m, 1H), 1.69(m, 2H), 1.60(t, J = 6.0 Hz, 2H), 1.37(m, 4H), 1.03(t, J = 6.8 Hz, 3H). ^{13}C NMR(100 MHz, Acetone-d_6) δ 174.13, 171.52, 157.54, 142.48, 140.86, 139.44, 139.31, 138.49,

136.71, 129.30, 129.05, 128.99, 128.55, 128.10, 127.35, 125.81, 123.75, 122.95, 119.25, 119.04, 115.67, 115.44, 84.16, 82.62, 61.86, 36.72, 33.32, 30.49, 30.33, 29.65, 28.44, 25.24, 25.21, 24.60, 20.34; HRMS(ESI) calcd for $C_{35}H_{39}N_2O_7S$ [M - H]$^-$, 647.2478; found 631.2483.

8-(4-(6-(*N*-Ethyl-*N*-(4-methoxyphenyl)sulfamoyl)-3-(4-hydroxyphenyl)-7-oxabicyclo [2.2.1] hept-2-en-2-yl)phenylamino)-8-oxooctanoic acid (17d). Pale yellow solid, 91% yield, m.p. 141–143 °C; ^{1}H NMR(400 MHz, Acetone-d_6) δ 9.16(s, 1H, —CONH—), 7.50(d, J = 8.8 Hz, 1H), 7.46(d, J = 8.8 Hz, 1H), 7.12(d, J = 8.4 Hz, 2H), 7.11(d, J = 8.0 Hz, 2H), 7.09(d, J = 8.4 Hz, 1H), 7.06(d, J = 8.0 Hz, 1H), 6.72(d, J = 8.8 Hz, 2H), 6.70(d, J = 8.8 Hz, 1H), 6.66(d, J = 8.4 Hz, 1H), 5.35(s, 1H), 5.20(s, 1H), 3.64(m, 2H), 3.62(s, 3H), 3.37(m, 1H), 2.23(m, 2H), 2.14(t, J = 6.8 Hz, 2H), 2.07(m, 1H), 1.91(m, 1H), 1.54(m, 2H), 1.45(t, J = 6.4 Hz, 2H), 1.23(m, 4H), 0.88(t, J = 7.2 Hz, 3H). ^{13}C NMR(100 MHz, Acetone-d_6) δ 175.10, 172.48, 159.91, 158.40, 143.10, 141.52, 140.11, 139.95, 138.05, 132.56, 131.50, 130.18, 129.55, 128.99, 128.36, 124.96, 124.29, 120.39, 120.16, 116.66, 116.46, 115.00, 85.32, 83.64, 62.13, 55.80, 47.36, 37.72, 34.25, 31.36, 31.18, 26.16, 25.54, 20.64, 14.97

8-(4-(6-(*N*-Ethyl-*N*-(3-methoxyphenyl)sulfamoyl)-3-(4-hydroxyphenyl)-7-oxabicyclo [2.2.1] hept-2-en-2-yl)phenylamino)-8-oxooctanoic Acid (17e). Pale yellow solid, 94% yield, m.p. 145–148 °C; ^{1}H NMR(400 MHz, Acetone-d_6) δ 9.15(s, 1H, —CONH—), 7.48(d, J = 8.8 Hz, 2H), 7.12(t, J = 8.0 Hz, 3H), 7.06(d, J = 8.0 Hz, 2H), 6.82(d, J = 8.0 Hz, 2H), 6.73(d, J = 8.4 Hz, 1H), 6.66(d, J = 8.8 Hz, 2H), 5.37(s, 1H), 5.19(s, 1H), 3.70(m, 2H), 3.60(s, 3H), 3.42(m, 1H), 2.23(m, 2H), 2.14(t, J = 7.2 Hz, 2H), 2.05(m, 1H), 1.91(m, 1H), 1.54(m, 2H), 1.45(t, J = 6.8 Hz, 2H), 1.23(m, 4H), 0.90(t, J = 6.8 Hz, 3H). ^{13}C NMR (100 MHz, Acetone-d_6) δ 175.08, 172.46, 161.04, 158.42, 143.22, 141.42, 139.98, 139.71, 138.02, 130.47, 130.02, 129.63, 128.81, 128.42, 124.94, 124.25, 121.77, 120.30, 116.64, 116.46, 115.93, 113.86, 85.24, 83.68, 62.66, 55.75, 47.03, 37.72, 34.24, 32.67, 31.18, 26.15, 25.54, 20.63, 14.94; HRMS(ESI) calcd for $C_{35}H_{39}N_2O_8S$ [M - H]$^-$, 647.2428; found 647.2433.

8-(4-(-6-(*N*-(4-Hydroxyphenyl)-*N*-ethylsulfamoyl)-3-(4-hydroxyphenyl)-7-oxabicyclo [2.2.1] hept-2-en-2-yl)phenylamino)-8-oxooctanoic acid (17f). Pale yellow solid, 93% yield, m.p. 151–153 °C; ^{1}H NMR(400 MHz, Acetone-d_6) δ 9.35(s, 1H, —CONH—), 7.66(d, J = 8.0 Hz, 2H), 7.29(d, J = 8.8 Hz, 2H), 7.22(d, J = 8.8 Hz, 2H), 7.15(d, J = 8.8 Hz, 2H), 6.81(d, J = 8.4 Hz, 2H), 6.77(d, J = 8.0 Hz, 2H), 5.49(s, 1H), 5.35(t, J = 3.6 Hz, 1H), 3.76(m, 2H), 3.53(m, 1H), 2.42(t, J = 7.2 Hz, 2H), 2.29(t, J = 7.2 Hz, 2H), 2.23(m, 1H), 2.06(m, 1H), 1.70(t, J = 7.6 Hz, 2H), 1.62(t, J = 6.8 Hz, 2H), 1.37(m, 4H), 1.02(t, J = 7.2 Hz, 3H). ^{13}C NMR(100 MHz, Acetone-d_6) δ 175.06, 172.48, 158.53, 157.83, 141.48, 139.94, 139.79, 131.68, 131.47, 130.17, 129.08, 128.37, 124.28, 120.12, 116.63, 116.45, 84.14, 83.58, 61.97, 47.38, 37.71, 34.24, 31.36, 30.70, 29.65, 26.15, 25.54, 14.90; HRMS(ESI) calcd for $C_{34}H_{37}N_2O_8S$ [M - H]$^-$, 633.2271; found 633.2276.

8-(4-(-6-(*N*-(3-Chlorophenyl)-*N*-ethylsulfamoyl)-3-(4-hydroxyphenyl)-7-oxabic-yclo [2.2.1] hept-2-en-2-yl)phenylamino)-8-oxooctanoic acid (17g). Pale yellow solid, 87% yield, m.p. 144–146 °C; ^{1}H NMR(400 MHz, Acetone-d_6) δ 9.29(s, 1H, —CONH—), 7.64(d, J = 8.8 Hz, 1H), 7.61(d, J = 8.8 Hz, 1H), 7.39(m, 4H), 7.27(d, J = 8.4 Hz, 1H), 7.25(d, J = 8.4 Hz, 1H), 7.22(d, J = 8.0 Hz, 1H), 7.20(d, J = 8.0 Hz, 1H), 6.82(d, J = 8.8 Hz, 1H), 6.78(d, J = 8.8 Hz, 1H), 5.52(s, 1H), 5.36 (s, 1H), 3.84(m, 2H), 3.56(m, 1H), 2.38(m, 2H), 2.29(t, J = 7.2 Hz, 2H), 2.13(m, 1H), 2.07(m, 1H), 1.70(m, 2H), 1.60(t, J = 6.4 Hz, 2H), 1.37(m, 4H), 1.03(t, J = 6.8 Hz, 3H). ^{13}C NMR(100 MHz, Acetone-d_6) δ 175.08, 172.49, 158.50, 143.36, 141.77, 140.11, 139.84, 138.13, 137.27, 135.81, 134.24, 131.36, 130.73, 129.63, 128.60, 128.40, 124.97, 124.28, 120.27, 120.15, 116.62, 116.47, 85.48, 83.70, 63.85, 47.09, 37.73, 34.23, 29.67, 26.20, 26.16, 25.54, 20.66, 14.64; HRMS(ESI) calcd for $C_{34}H_{36}ClN_2O_7S$ [M - H]$^-$, 651.1932; found 651.1937.

8-(4-(-6-(*N*-(4-chlorophenyl)-*N*-ethylsulfamoyl)-3-(4-hydroxyphenyl)-7-oxabicyclo [2.2.1] hept-2-en-2-yl)phenylamino)-8-oxooctanoic acid (17h). Pale yellow solid, 90% yield, m.p. 141–143 °C; ^{1}H NMR(400 MHz, Acetone-d_6) δ 9.28(s, 1H, —CONH—), 7.66(d, J = 8.4 Hz, 2H), 7.51(d, J = 8.8 Hz, 2H), 7.37(d, J = 8.0 Hz, 2H), 7.27(d, J = 8.4 Hz, 2H), 7.24(d, J = 8.8 Hz, 2H), 6.84(d, J = 8.4 Hz, 2H), 5.58(s, 1H), 5.38(s, 1H), 3.68(m, 3H), 2.39(t, J = 7.6 Hz, 3H), 2.29(t, J = 7.2 Hz, 2H), 2.27(m, 1H), 1.69(t, J = 6.8 Hz, 2H), 1.60(t, J = 7.2 Hz, 2H), 1.37(m, 4H), 1.05(t, J = 7.2 Hz, 3H). ^{13}C NMR(100 MHz, Acetone-d_6) δ 175.21, 172.53, 158.53, 143.17, 141.57, 139.98, 139.18, 137.90, 133.55, 131.63, 131.59, 130.11, 129.95, 129.64, 128.89, 128.43, 124.86, 124.21, 120.36, 120.16, 116.64, 116.45, 85.25, 83.63, 62.68, 47.04, 37.73, 34.12, 31.38, 31.18, 29.67, 26.17, 25.54, 14.84; HRMS (ESI) calcd for $C_{34}H_{36}ClN_2O_7S$ [M - H]$^-$, 651.1932; found 651.1937.

8-(4-(6-(*N*-(2-bromophenyl)-*N*-ethylsulfamoyl)-3-(4-hydroxyphenyl)-7-oxabicyclo [2.2.1] hept-2-en-2-yl)phenylamino)-8-oxooctanoic acid (17i). Pale yellow solid, 89% yield, m.p. 145–147 °C; ^{1}H NMR(400 MHz, Acetone-d_6) δ 9.25(s, 1H, —CONH—), 7.65(d, J = 8.0 Hz, 3H), 7.35(m, 2H), 7.29(d, J = 8.4 Hz, 3H), 7.21(d, J = 8.0 Hz, 2H), 6.83(d, J = 8.8 Hz, 2H), 5.61(s, 1H), 5.39(t, J = 3.2 Hz, 1H), 3.84 (m, 1H), 3.70(m, 2H), 2.40(t, J = 7.2 Hz, 2H), 2.30(t, J = 7.6 Hz, 2H), 2.20(m, 1H), 2.07(m, 1H), 1.70(t, J = 6.4 Hz, 2H), 1.61(t, J = 6.8 Hz, 2H), 1.39(m, 4H), 1.08(t, J = 6.8 Hz, 3H). ^{13}C NMR(100 MHz, Acetone-d_6) δ 174.16, 171.55, 157.67, 142.17, 140.54, 139.08, 138.79, 137.36, 136.62, 129.55, 128.98, 128.64, 127.96, 127.43, 123.91, 123.23, 119.34, 119.15, 115.68, 115.50, 84.38, 82.64, 61.28, 46.21, 36.77, 33.35, 28.73, 25.23, 24.62, 20.15, 19.76, 14.02; HRMS(ESI) calcd for $C_{34}H_{36}BrN_2O_7S$ [M - H]$^-$, 695.1427; found 695.1432.

8-((4-(-3-(4-Hydroxyphenyl)-6-(*N*-phenyl-*N*-(2,2,2-trifluoroethyl)sulfamoyl)-7-oxabicyclo [2.2.1] hept-2-en-2-yl)phenyl) amino)-8-oxooctanoic acid (18a). Pale yellow solid, 97% yield, m.p. 122–125 °C; ^{1}H NMR(400 MHz, Acetone-d_6) δ 9.33(s, 1H, —CONH—), 7.64(d, J = 8.8 Hz, 1H), 7.61(d, J = 8.8 Hz, 1H), 7.46(t, J = 8.4 Hz, 2H), 7.35(m, 3H), 7.25(d, J = 8.0 Hz, 1H), 7.23(d, J = 8.4 Hz, 1H), 7.20(d, J = 8.0 Hz, 1H), 7.19(d, J = 8.0 Hz, 1H), 6.85(d, J = 8.8 Hz, 1H), 6.81(d, J = 8.4 Hz, 1H), 5.56(s, 1H), 5.36(s, 1H), 4.59(m, 2H), 3.63(m, 1H), 2.37 (t, J = 7.6 Hz, 2H), 2.28(m, 2H), 2.15(m, 1H), 2.06(m, 1H), 1.68(t, J = 7.2 Hz, 2H), 1.60(m, 2H), 1.37(m, 4H). ^{13}C NMR(100 MHz, Acetone-d_6) δ 174.91, 172.24, 158.56, 143.32, 141.80, 140.50, 139.40, 137.73, 130.21, 129.87, 129.82, 129.53, 129.19, 129.01, 128.72, 128.32, 128.09, 124.75, 124.05, 120.15, 119.92, 116.57, 116.37, 85.18, 83.57, 63.01, 37.63, 34.17, 31.41, 31.25, 29.64, 29.56, 26.09, 25.51; HRMS (ESI) calcd for $C_{34}H_{34}F_3N_2O_7S$ [M - H]$^-$, 671.2039; found 671.2044.

8-(4-(3-(4-Hydroxyphenyl)-6-(*N*-(m-tolyl)-*N*-(2,2,2-trifluoroethyl)sulfamoyl)-7-oxabicyclo [2.2.1] hept-2-en-2-yl)phenylamino)-8-oxooctanoic acid (18b). Pale yellow solid, 95% yield, m.p. 124–126 °C; ^{1}H NMR(400 MHz, Acetone-d_6) δ 9.29(s, 1H, —CONH—), 7.64(m, 2H), 7.30(d, J = 8.0 Hz, 2H), 7.21(d, J = 8.4 Hz, 2H), 7.21(m, 2H), 7.12(d, J = 8.4 Hz, 1H), 7.08(d, J = 8.4 Hz, 1H), 6.85(d, J = 8.4 Hz, 1H), 6.82(d, J = 8.4 Hz, 1H), 5.56(s, 1H), 5.36(s, 1H), 4.51(m, 2H), 3.63 (m, 1H), 2.39(t, J = 7.6 Hz, 2H), 2.33(m, 2H), 2.31(m, 3H), 2.18(m, 1H), 1.98(m, 1H), 1.70(t, J = 6.4 Hz, 2H), 1.60(t, J = 6.4 Hz, 2H), 1.38(m, 4H). ^{13}C NMR(100 MHz, Acetone-d_6) δ 175.28, 172.67, 157.61, 143.40, 141.49, 140.14, 139.27, 137.81, 131.18, 130.79, 130.55, 130.28, 129.53, 129.09, 126.55, 126.36, 124.77, 124.09, 120.21, 116.67, 116.48, 116.24, 85.24, 83.56, 62.86, 37.75, 34.27, 29.66, 26.22, 26.20, 26.17, 25.54, 21.11, 20.68; HRMS(ESI) calcd for $C_{35}H_{36}F_3N_2O_7S$ [M - H]$^-$, 685.2206; found 685.2201.

8-(4-(3-(4-Hydroxyphenyl)-6-(*N*-(m-tolyl)-*N*-(2,2,2-trifluoroethyl)sulfamoyl)-7-oxabicyclo [2.2.1] hept-2-en-2-yl)phenylamino)-8-oxooctanoic acid (18c). Pale yellow solid, 94% yield, m.p. 123–125 °C; ^{1}H NMR(400 MHz, Acetone-d_6) δ 9.27(s, 1H, —CONH—), 7.66(d, J = 8.0 Hz, 1H), 7.61(d, J = 8.0 Hz, 1H), 7.35(m, 1H), 7.27(d, J = 8.8 Hz, 2H), 7.24(d, J = 8.4 Hz, 2H), 7.22(m, 2H), 7.05(t, J = 8.0 Hz, 1H), 6.86(d, J = 8.8 Hz, 1H), 6.81(d, J = 8.8 Hz, 1H), 5.59(s, 1H), 5.36 (s, 1H), 4.58(m, 2H), 3.63(m, 1H), 2.38(t, J = 7.2 Hz, 2H), 2.30(m, 2H), 2.27(s, 3H), 2.21(m, 1H), 2.10(m, 1H), 1.70(t, J = 6.4 Hz, 2H), 1.62(m, 2H), 1.40(m, 4H). ^{13}C NMR(100 MHz, Acetone-d_6) δ 175.00, 172.45, 158.47, 143.10, 141.55, 140.03, 139.58, 137.90, 129.99, 129.85,

129.68, 128.77, 128.47, 127.74, 127.42, 127.35, 124.84, 124.23, 120.26, 120.10, 116.58, 116.42, 85.21, 83.60, 61.48, 39.23, 39.13, 37.71, 34.22, 31.33, 31.14, 29.66, 26.14, 25.54; HRMS(ESI) calcd for $C_{35}H_{36}F_3N_2O_7S$ [M - H]$^-$, 685.2206; found 685.2201.

8-(4-(3-(4-Hydroxyphenyl)-6-(*N*-(p-tolyl)-*N*-(2,2,2-trifluoroethyl)sulfamoyl)-7-oxabicyclo[2.2.1]hept-2-en-2-yl)phenylamino)-8-oxooctanoic acid (18d). Pale yellow solid, 95% yield, m.p. 126–128 °C; ^{1}H NMR(400 MHz, Acetone-d_6) δ 9.32(s, 1H, —CONH—), 7.68(d, J = 8.4 Hz, 1H), 7.63(d, J = 8.4 Hz, 1H), 7.35(d, J = 8.8 Hz, 2H), 7.30(d, J = 8.0 Hz, 1H), 7.26(d, J = 8.0 Hz, 1H), 7.21(d, J = 8.8 Hz, 1H), 7.18(d, J = 8.8 Hz, 1H), 6.85(d, J = 8.0 Hz, 1H), 6.84(d, J = 8.4 Hz, 2H), 6.79(d, J = 8.4 Hz, 1H), 5.54(s, 1H), 5.37(s, 1H), 4.52(m, 2H), 3.76(s, 3H), 3.61(m, 1H), 2.39(t, J = 7.2 Hz, 2H), 2.30(t, J = 7.2 Hz, 2H), 2.21 (m, 1H), 2.06(m, 1H), 1.69(t, J = 6.4 Hz, 2H), 1.60(m, 2H), 1.37(m, 4H). ^{13}C NMR(100 MHz, Acetone-d_6) δ 175.44, 172.86, 160.39, 158.41, 143.30, 141.76, 140.09, 139.55, 137.70, 132.68, 131.32, 131.30, 130.39, 129.50, 129.21, 128.31, 124.77, 124.07, 120.56, 120.31, 116.69, 115.29, 85.26, 83.64, 62.44, 55.87, 37.76, 37.71, 34.29, 31.45, 29.57, 26.20, 25.53, 20.71; HRMS(ESI) calcd for $C_{35}H_{36}F_3N_2O_8S$ [M - H]$^-$, 701.2155; found 701.2150.

8-((4-(-3-(4-Hydroxyphenyl)-6-(*N*-(3-methoxyphenyl)-*N*-(2,2,2-trifluoroethyl)s-ulfamoyl)-7-ox-abicyclo[2.2.1]hept-2-en-2-yl)phenyl)amino)-8-oxooctanoic acid (18e). Pale yellow solid, 96% yield, m.p. 123–126 °C; ^{1}H NMR(400 MHz, Acetone-d_6) δ 7.52(d, J = 8.4 Hz, 1H), 7.47(d, J = 8.4 Hz, 1H), 7.12(d, J = 8.0 Hz, 3H), 7.06(d, J = 8.0 Hz, 1H), 7.04(d, J = 8.0 Hz, 1H), 6.94(m, 2H), 6.79(d, J = 8.4 Hz, 1H), 6.70(d, J = 8.4 Hz, 1H), 6.64(d, J = 8.8 Hz, 1H), 5.43(s, 1H), 5.22 (s, 1H), 4.46(m, 2H), 3.62(s, 3H), 3.49(m, 1H), 2.26(t, J = 6.8 Hz, 2H), 2.14(t, J = 7.2 Hz, 3H), 2.06(m, 1H), 1.56(m, 2H), 1.46(m, 2H), 1.37(m, 4H). ^{13}C NMR(100 MHz, Acetone-d_6) δ 175.10, 172.57, 161.16, 158.45, 143.49, 141.54, 139.93, 139.45, 137.68, 130.87, 130.12, 129.57, 128.91, 128.36, 124.68, 123.94, 121.47, 120.24, 120.06, 116.56, 116.38, 115.56, 114.63, 85.18, 83.59, 63.07, 55.82, 37.65, 34.22, 31.49, 31.32, 30.57, 26.16, 26.14, 25.51; HRMS(ESI) calcd for $C_{35}H_{36}F_3N_2O_8S$ [M - H]$^-$, 701.2155; found 701.2150.

8-(4-(6-(*N*-Benzyl-*N*-(2,2,2-trifluoroethyl)sulfamoyl)-3-(4-hydroxyphenyl)-7-ox-abicyclo[2.2.1]hept-2-en-2-yl)phenyl)amino)-8-oxooctanoic acid (18f). Pale yellow solid, 94% yield, m.p. 127–129 °C; ^{1}H NMR(400 MHz, Acetone-d_6) δ 9.28(s, 1H, —CONH—), 7.66(d, J = 8.0 Hz, 2H), 7.38(m, 2H), 7.32(d, J = 8.0 Hz, 2H), 7.29(d, J = 8.0 Hz, 1H), 7.27(d, J = 8.4 Hz, 1H), 7.25(d, J = 8.0 Hz, 1H), 7.22(d, J = 8.4 Hz, 1H), 7.09(d, J = 8.4 Hz, 1H), 6.84(d, J = 8.4 Hz, 2H), 5.62(s, 1H), 5.41(s, 1H), 4.67(m, 2H), 4.00(m, 2H), 3.58(m, 1H), 2.40(m, 3H), 2.30(t, J = 7.6 Hz, 2H), 2.06(m, 1H), 1.71(t, J = 6.0 Hz, 2H), 1.61(t, J = 6.8 Hz, 2H), 1.39(m, 4H). ^{13}C NMR(100 MHz, Acetone-d_6) δ 179.64, 177.04, 162.89, 147.72, 145.99, 144.31, 144.07, 142.29, 140.51, 134.83, 134.83, 134.31, 134.01, 133.91, 133.84, 133.32, 133.08, 132.78, 129.01, 128.27, 124.56, 120.93, 120.54, 89.34, 88.00, 57.77, 42.04, 38.63, 35.74, 35.51, 35.04, 30.50, 29.85, 25.05; HRMS(ESI) calcd for $C_{35}H_{36}F_3N_2O_7S$ [M - H]$^-$, 685.2205; found 685.2201.

4.3. Estrogen receptor binding affinity

Relative binding affinities were determined by a competitive fluorometric binding assay. Briefly, 40 nM fluorescence tracer (coumestrol, Sigma-Aldrich, MO) and 0.8 μM purified human ERα or ERβ ligand binding domain (LBD) were diluted in 100 mM potassium phosphate buffer (pH 7.4), containing 100 μg/mL bovine gamma globulin (Sigma-Aldrich, MO). Incubations were for 2 h at room temperature (25 ℃) in dark place. Then fluorescence polarization values were measured using Cytation 3 microplate reader. The binding affinities are expressed as relative binding affinity (RBA) values with the RBA of 17β-estradiol set to 100%. The values given are the average ± range of two independent determinations. IC_{50} values were calculated according to equations described previously.[41,47]

4.4. Gene transcriptional activity

The human embryonic kidney cell lines, HEK 293T, was cultured in Dulbecco's Minimum Essential Medium (DMEM) (Gibco by Invitrogen Corp., CA) with 10% fetal bovine serum (FBS) (Hylcone by Thermo Scientific, UT). Cells were plated in phenol red-free DMEM with 10% FBS. HEK 293T cells were transfected with 25 μL mixture per well, containing 300 ng of 3 × ERE-luciferase reporter, 100 ng of ERα or ERβ expression vector, 125 mM calcium chloride (GuoYao, China) and 12.5 μL 2 × HBS. The next day, the cells were treated with increasing doses of ER ligands diluted in phenol red free DMEM with 10% FBS. After 24 h, luciferase activity was measured using Dual-Luciferase Reporter Assay System (Promega,MI) according to the manufacturer's protocol.[48]

4.5. Cell culture and cell viability assay

Human breast cancer cell lines MCF-7, Human prostate cancer cell DU145 and African green monkey kidney cell lines VERO were obtained from cell bank of Chinese Academy of Science (Shanghai, China). Cells were cultured in DMEM with 10% FBS, 100U/ml penicillin, 100U/ml streptomycin and maintained at 37 ℃ in a 5% CO_2 humidifier incubator. For cell viability experiments, cells were grown in 96-well microtiter plates (Nest Biotech Co., China) with appropriate ligand triplicate for 72 h. MTT colormetric tests (Biosharp, China) were employed to determine cell viability per manufacturer instructions. IC_{50} values were calculated according to the following equation using Origin software: Y = 100% inhibition + (0% inhibition-100% inhibition)/(1 + $10^{[(LogIC50-X)\times Hill\text{-}slope]}$), where Y = fluorescence value, X = Log[*inhibitor*].[49]

4.6. Western blot assay

After being treaterd with DMSO, fulvestrant (20 μM), SAHA (10 μM) or conjugate (20 μM) for 24 h, cell plated in 6-well plate were washed twice with ice-cold PBS and extracted with RIPA (Beyotime Biotechnology, China) containing 1% PMSF and 1% phosphatase inhibitor cocktail solution ((Beyotime Biotechnology, China) on ice for 30 min. The cell lysates were boiled for 10 min in sodium dodecyl sulfate (SDS) gel-loading buffer and then stored at − 20 ℃ for Western blot analysis Proteins from cell lysates were separated on 8% or 10% SDS-PAGE gels and then transferred to polyvinylidene fluoride (PVDF) membranes (Millipore, USA). The membrans were blocked with 5% non-fat milk for 1 h at room temperature and incubated with indicated antibodies overnight at 4 ℃. The next day, membranes were incubated with HRP-conjugated secondary antibodies diluted in 5% non-fat milk at room temperature for 1 h. At last, protein bands were detected by using ECL chemiluminescence kit (Millipore, USA).[50] The primary antibodies used include: Anti-acetyl α-tubulin (catalog ab179484, 1:4000 dilution) was from Abcam (Cambridge, UK). Anti-ERα (catalog #8644, 1:1000 dilution), anti-α-tubulin (catalog #2144, 1:800 dilution), anti-histone H3 (catalog #9715, 1:10000 dilution), anti-acetyl histone H3 (catalog #9649, 1:10000 dilution), were from Cell Signaling Technology (Danvers, USA). Anti-β-actin (catalog A8481, 1:6000 dilution) was from Sigma-Aldrich (St, Louis, USA). Secondary goat anti-mouse (catalog #2305) and anti-rabbit (catalog #2301) horseradish peroxidase (HRP) antibodies were obtained from Wuhan Feiyi Group (Wuhan, China).

4.7. HDAC activity assay

In vitro HDAC activity was measured using Fluorogenic HDAC8 and HDAC6 Assay Kit (BPS Bioscience, CA) according to the manufacturer's protocol. All of the tested compounds were prepared in DMSO and were diluted in HDAC assay buffer to different concentration. The enzymatic reactions were conducted in duplicate at 37 ℃ for 30 min in a 50 μL mixture containing HDAC assay buffer, 5 μg of BSA, HDAC substrate, HDAC enzyme (human recombinant HDAC8, HDAC6), and various concentrations of tested compound. Then, 50 μL of 2 × HDAC Developer

was added to each well and the plate was incubated at room temperature for 15 min. Fluorescence values were measured at an excitation of 380 nm and an emission of 460 nm using Cytation 3 microplate reader. IC_{50} values were calculated according to the following equation using Origin software: $Y = F_b + (F_t - F_b)/(1 + 10^{[(LogIC50-X) \times Hillslope]})$, where Y = fluorescence value, F_b = minimum fluorescence value, F_t = maximum fluorescence value, X = Log[*inhibitor*].[48]

Declaration of Competing Interest

The authors declare that they have no known competing financial interests or personal relationships that could have appeared to influence the work reported in this paper.

Acknowledgements

We are grateful to the NSFC (81773557, 31870786, 82073690), the Fundamental Research Funds for the Central Universities of China (2042020kf1043), and the Seed Funds for International Joint Research Platform of Wuhan University (KYPT-ZD-9) for support of this research for support of this research.

Appendix A. Supplementary material

Supplementary data to this article can be found online at https://doi.org/10.1016/j.bmc.2021.116185.

References

1 de Deus Moura R, Carvalho FM, Bacchi CE. Breast cancer in very young women: Clinicopathological study of 149 patients ≤25 years old. *Breast*. 2015;24:461–467.
2 Harbeck N, Penault-Llorca F, Cortes J, et al. Breast cancer. *Nat Rev Dis Primers*. 2019;5:66.
3 Siegel RL, Miller KD, Jemal A. Cancer statistics, 2020. *CA Cancer J Clin*. 2020;70:7–30.
4 DeSantis CE, Ma J, Gaudet MM, et al. Breast cancer statistics, 2019. *CA Cancer J Clin*. 2019;69:438–451.
5 Ariazi EA, Ariazi JL, Cordera F, Jordan VC. Estrogen receptors as therapeutic targets in breast cancer. *Curr Top Med Chem*. 2006;6:181–202.
6 Craig Jordan V, McDaniel R, Agboke F, Maximov PY. The evolution of nonsteroidal antiestrogens to become selective estrogen receptor modulators. *Steroids*. 2014;90:3–12.
7 Shea MP, O'Leary KA, Fakhraldeen SA, et al. Antiestrogen therapy increases plasticity and cancer stemness of prolactin-induced ERa þ mammary carcinomas. *Cancer Res*. 2018;78:1672–1684.
8 Lai A, Kahraman M, Govek S, et al. Identification of GDC-0810 (ARN-810), an Orally Bioavailable Selective Estrogen Receptor Degrader (SERD) that Demonstrates Robust Activity in Tamoxifen-Resistant Breast Cancer Xenografts. *J Med Chem*. 2015;58:4888–4904.
9 Paplomata E, O'Regan R. New and emerging treatments for estrogen receptor-positive breast cancer: focus on everolimus. *Ther Clin Risk Manag*. 2013;9:27–36.
10 Zardavas D, Baselga J, Piccart M. Emerging targeted agents in metastatic breast cancer. *Nat Rev Clin Oncol*. 2013;10:191–210.
11 Schiff R, Massarweh S, Shou J, Osborne CK. Breast Cancer Endocrine Resistance. *How Growth Factor Signal Estrogen Receptor Coregul Modul Resp*. 2003;9:447s–454s.
12 Group, E. B. C. T. C. Relevance of breast cancer hormone receptors and other factors to the efficacy of adjuvant tamoxifen: patient-level meta-analysis of randomised trials. *The Lancet*. 2011;378:771–784.
13 Jordan VC. Tamoxifen: A most unlikely pioneering medicine. *Nat Rev Drug Discovery*. 2003;2:205–213.
14 van Leeuwen FE, van den Belt-Dusebout AW, van Leeuwen FE, et al. Risk of endometrial cancer after tamoxifen treatment of breast cancer. *The Lancet*. 1994;343:448–452.
15 Shang Y, Brown M. Molecular determinants for the tissue specificity of SERMs. *Science*. 2002;295:2465–2468.
16 Lewis JS, Jordan VC. Selective estrogen receptor modulators (SERMs): Mechanisms of anticarcinogenesis and drug resistance. *Mutat Res - Fund Mole Mech Mutag*. 2005;591:247–263.
17 Vogel VG. The NSABP study of tamoxifen and raloxifene (STAR) trial. *Expert Rev Anticancer Ther*. 2009;9:51–60.
18 Fagerlin A, Zikmund-Fisher BJ, Smith DM, et al. Women's decisions regarding tamoxifen for breast cancer prevention: responses to a tailored decision aid. *Breast Cancer Res Treat*. 2010;119:613–620.
19 Zheng Y, Luo J, Bao P, et al. Long-term cognitive function change among breast cancer survivors. *Breast Cancer Res Treat*. 2014;146:599–609.
20 Abdel-Magid AF. Selective estrogen receptor degraders (SERDs): A promising treatment to overcome resistance to endocrine therapy in ERα-positive breast cancer. *ACS Med Chem Lett*. 2017;8:1129–1131.
21 Hu X, Veroni M, De Luise M, et al. Circumvention of tamoxifen resistance by the pure anti-estrogen ICI 182, 780. *Int J Cancer*. 1993;55:873–876.
22 Mehta RS, Barlow WE, Albain KS, et al. Combination anastrozole and fulvestrant in metastatic breast cancer. *N Engl J Med*. 2012;367:435–444.
23 Carlson RW. The history and mechanism of action of fulvestrant. *Clin Breast Cancer*. 2005;6:5–8.
24 Nathan MR, Schmid P. A review of fulvestrant in breast cancer. *Oncol Ther*. 2017;5:17–29.
25 Zhou HB, Comninos JS, Stossi F, Katzenellenbogen BS, Katzenellenbogen JA. Synthesis and evaluation of estrogen receptor ligands with bridged oxabicyclic cores containing a diarylethylene motif: Estrogen antagonists of unusual structure. *J Med Chem*. 2005;48:7261–7274.
26 Zhu M, Zhang C, Nwachukwu JC, et al. Bicyclic core estrogens as full antagonists: Synthesis, biological evaluation and structure-activity relationships of estrogen receptor ligands based on bridged oxabicyclic core arylsulfonamides. *Org Biomol Chem*. 2012;10:8692–8700.
27 Srinivasan S, Nwachukwu JC, Bruno NE, et al. Full antagonism of the estrogen receptor without a prototypical ligand side chain. *Nat Chem Biol*. 2017;13:111–118.
28 Li Y, Zhang S, Zhang J, et al. Exploring the PROTAC degron candidates: OBHSA with different side chains as novel selective estrogen receptor degraders (SERDs). *Eur J Med Chem*. 2019;172:48–61.
29 Hu Z, Li Y, Xie B, et al. Novel class of 7-Oxabicyclo[2.2.1]heptene sulfonamides with long alkyl chains displaying improved estrogen receptor alpha degradation activity. *Eur J Med Chem*. 2019;182:111605.
30 Darb-Esfahani S, Denkert C, Stenzinger A, et al. Role of TP53 mutations in triple negative and HER2-positive breast cancer treated with neoadjuvant anthracycline/taxane-based chemotherapy. *Oncotarget*. 2016;7:67686–67698.
31 Chen Y, Olopade OI. MYC in breast tumor progression. *Expert Rev Anticancer Ther*. 2008;8:1689–1698.
32 Elizalde PV, Cordo Russo RI, Chervo MF, Schillaci R. ErbB-2 nuclear function in breast cancer growth, metastasis and resistance to therapy. *Endocr Relat Cancer*. 2016;23:T243–T257.
33 Sun YS, Zhao Z, Yang ZN, et al. Risk Factors and Preventions of Breast Cancer. *Int J Biol Sci*. 2017;13:1387–1397.
34 Deng CX. BRCA1: cell cycle checkpoint, genetic instability, DNA damage response and cancer evolution. *Nucleic Acids Res*. 2006;34:1416–1426.
35 Ning W, Hu Z, Tang C, et al. Novel Hybrid Conjugates with Dual Suppression of Estrogenic and Inflammatory Activities Display Significantly Improved Potency against Breast Cancer. *J Med Chem*. 2018;61:8155–8173.
36 Tang Z, Wu C, Wang T, et al. Design, synthesis and evaluation of 6-aryl-indenoisoquinolone derivatives dual targeting ERalpha and VEGFR-2 as anti-breast cancer agents. *Eur J Med Chem*. 2016;118:328–339.
37 McDermott MSJ, Canonici A, Ivers L, et al. Dual inhibition of IGF1R and ER enhances response to trastuzumab in HER2 positive breast cancer cells. *Int J Oncol*. 2017;50:2221–2228.
38 Verma AK, Fatima K, Dudi RK, et al. Antiproliferative activity of diarylnaphthylpyrrolidine derivative via dual target inhibition. *Eur J Med Chem*. 2020;188:111986.
39 Kastrati I, Siklos MI, Brovkovych SD, Thatcher GRJ, Frasor J. A Novel Strategy to Co-target Estrogen Receptor and Nuclear Factor kappaB Pathways with Hybrid Drugs for Breast Cancer Therapy. *Hormones Cancer*. 2017;8:135–142.
40 Gryder BE, Rood MK, Johnson KA, et al. Histone deacetylase inhibitors equipped with estrogen receptor modulation activity. *J Med Chem*. 2013;56:5782–5796.
41 Tang C, Li C, Zhang S, et al. Novel Bioactive Hybrid Compound Dual Targeting Estrogen Receptor and Histone Deacetylase for the Treatment of Breast Cancer. *J Med Chem*. 2015;58:4550–4572.
42 Schafer C, Goder A, Beyer M, et al. Class I histone deacetylases regulate p53/NF-kappaB crosstalk in cancer cells. *Cell Signal*. 2017;29:218–225.
43 Gui CY, Ngo L, Xu WS, Richon VM, Marks PA. Histone deacetylase (HDAC) inhibitor activation of p21WAF1 involves changes in promoter-associated proteins, including HDAC1. *Proc Natl Acad Sci U S A*. 2004;101:1241–1246.
44 Saji S, Kawakami M, Hayashi S, et al. Significance of HDAC6 regulation via estrogen signaling for cell motility and prognosis in estrogen receptor-positive breast cancer. *Oncogene*. 2005;24:4531–4539.
45 Park SY, Jun JIAE, Jeong KJ, et al. Histone deacetylases 1, 6 and 8 are critical for invasion in breast cancer. *Oncol Rep*. 2011;25:1677–1681.
46 Samavat H, Kurzer MS. Estrogen metabolism and breast cancer. *Cancer Lett*. 2015;356:231–243.
47 Wang C, Li C, Zhou H, Huang J. High-throughput screening assays for estrogen receptor by using coumestrol, a natural fluorescence compound. *J Biomol Screen*. 2014;19:253–258.
48 Li C, Tang C, Hu Z, et al. Synthesis and structure-activity relationships of novel hybrid ferrocenyl compounds based on a bicyclic core skeleton for breast cancer therapy. *Bioorg Med Chem*. 2016;24:3062–3074.
49 Wu J, Yan J, Fang P, Zhou HB, Liang K, Huang J. Three-dimensional oxabicycloheptene sulfonate targets the homologous recombination and repair programmes through estrogen receptor alpha antagonism. *Cancer Lett*. 2020;469:78–88.
50 Xie H, Xiao Z, Huang J. C6 Glioma-Secreted NGF and FGF2 Regulate Neuronal APP Processing Through Up-Regulation of ADAM10 and Down-Regulation of BACE1, Respectively. *J Mole Neurosci: MN*. 2016;59:334–342.